JOURNAL OF THE AMERICAN WATER RESOURCES ASSOCIATION

AMERICAN WATER RESOURCES ASSOCIATION

ASSESSMENT OF ALTERNATIVE METHODS FOR STATISTICALLY DOWNSCALING DAILY GCM PRECIPITATION OUTPUTS TO SIMULATE REGIONAL STREAMFLOW[1]

Syewoon Hwang and Wendy D. Graham[2]

ABSTRACT: This study applied three statistical downscaling methods: (1) bias correction and spatial disaggregation at daily time scale (BCSD_daily); (2) a modified version of BCSD which reverses the order of spatial disaggregation and bias correction (SDBC), and (3) the bias correction and stochastic analog method (BCSA) to downscale general circulation model daily precipitation outputs to the subbasin scale for west-central Florida. Each downscaled climate input dataset was then used in an integrated hydrologic model to examine differences in ability to simulate retrospective streamflow characteristics. Results showed the BCSD_daily method consistently underestimated mean streamflow because the highly spatially correlated small precipitation events produced by this method resulted in overestimation of evapotranspiration. Highly spatially correlated large precipitation events produced by the SDBC method resulted in overestimation of the standard deviation of wet season daily streamflow and the magnitude/frequency of high streamflow events. BCSA showed better performance than the other methods in reproducing spatiotemporal statistics of daily precipitation and streamflow. This study demonstrated differences in statistical downscaling techniques propagate into significant differences in streamflow predictions, and underscores the need to carefully select a downscaling method that reproduces precipitation characteristics important for the hydrologic system under consideration.

(KEY TERMS: statistical downscaling; general circulation model (GCM); bias correction; spatiotemporal variability in daily precipitation; hydrologic implications; integrated hydrologic model (IHM).)

Hwang, Syewoon and Wendy D. Graham, 2014. Assessment of Alternative Methods for Statistically Downscaling Daily GCM Precipitation Outputs to Simulate Regional Streamflow. *Journal of the American Water Resources Association* (JAWRA) 1-23. DOI: 10.1111/jawr.12154

INTRODUCTION

General circulation models (GCMs) are effective tools for understanding present and past climate (Fowler *et al.*, 2007), and have been continually improved as understanding of the global system has advanced (Karl and Trenberth, 2003). However, the current generation of GCMs is not suitable for providing long-term simulation of atmospheric processes for precipitation and temperature at regional spatial scales because of intensive computational costs. It has been well documented that the resolution of the current generation of GCMs (>100 km) is not suitable for direct application to hydrologic and agricultural impact assessments (e.g., Christensen and Christensen, 2003; Wood *et al.*, 2004). The effective assessment of water resource impacts and adaptation strategies to climate change requires point scale (gauge based) or subbasin-based climate data to run

[1]Paper No. JAWRA-13-0068-P of the *Journal of the American Water Resources Association* (JAWRA). Received March 12, 2013; accepted November 18, 2013.

[2]Assistant Professor (Hwang), Department of Agricultural Engineering, Gyeongsang National University (Institute of Agriculture and Life Science), Jinju, South Korea 660-701 and Professor and Director (Graham), Water Institute, University of Florida, 570 Weil Hall, P.O. Box 116601, Gainesville, Florida 32611 (E-Mail/Hwang: swhwang78@gmail.com).

hydrologic models (Enke and Spekat, 1997; Andréasson *et al.*, 2004; Graham *et al.*, 2007; Leander *et al.*, 2008). This incongruity between the spatial resolution of GCMs and that needed by regional hydrologic models has been one of the major issues in developing reliable assessments of climate change impacts on water resources. This has led to a demand for improved downscaling techniques for better regional applications and evaluations (Feddersen and Andersen, 2005; Cañón *et al.*, 2011).

There are two categories of GCM downscaling: statistical downscaling methods which use empirical relationships between features simulated by GCMs at grid scales and surface observations at subgrid scales (Wilby and Wigley, 1997; Hay *et al.*, 2002) and dynamical downscaling techniques using regional climate models (RCMs) based on physical links between the climate at large and small scales (McGregor, 1997; Murphy, 1999). There have been numerous studies on the use of downscaling and bias correction methods to correct climate model outputs to produce realistic simulations of hydrological responses of the current climate (Mearns *et al.*, 1999; Zorita and von Storch, 1999; Widmann *et al.*, 2003; Diaz-Nieto and Wilby, 2005; Fowler *et al.*, 2007).

In general, dynamical downscaling has been shown to produce reasonable climate regimes that reflect temporal and spatial patterns of meteorological variables as RCMs provide physically coherent spatiotemporal variations in climate variables (Vasiliades *et al.*, 2009). However, the use of RCMs has significant computational cost and thus their routine application for the generation of ensembles of climate predictions using multiple GCMs and multiple scenarios is limited. Furthermore, RCMs have their own bias in addition to the bias propagated from boundary conditions and thus require bias correction prior to use for hydrologic, agricultural or natural resource impact assessments (Sato *et al.*, 2007; Hwang *et al.*, 2011, 2013).

On the other hand statistical downscaling methods can reduce the bias in climate data at high spatial resolution without the intensive computer resources required by dynamical downscaling (Iizumi *et al.*, 2011), and may thus be more amenable to climate impact research where analysis of multiple realizations of multiple climate models is required. For this reason, many studies have relied on statistical downscaling methods (e.g., Busuioc *et al.*, 2001; Charles *et al.*, 2004; Diaz-Nieto and Wilby, 2005). Although some statistical downscaling methods use various large-scale atmospheric variables as predictors (i.e., explanatory variables) to estimate local climatic elements (Wilby *et al.*, 1998; Wilby and Wigley, 2000), other studies have been devoted to developing and evaluating methods that directly use GCM daily precipitation as a predictor (e.g., Widmann *et al.*, 2003; Maurer and Hidalgo, 2008; Maurer *et al.*, 2010). However, simple statistical downscaling methods often fail to adequately reproduce spatial and temporal variability which is considered an important factor for predicting hydrologic response to climatic forcing (Beven and Hornberger, 1982; Milly and Eagleson, 1988). Accurately representing the spatiotemporal variability in precipitation events is important for accurately predicting regional hydrologic behavior, especially for low-relief, precipitation-driven subtropical regions affected by convective storms, as in Florida. For example, spatially uniform lower intensity rainfall typically produces higher evapotranspiration (ET) and more groundwater recharge over the domain and thus less surface runoff than more spatially distributed concentrated storms with the same total volume.

Recently, Hwang and Graham (2013) developed a stochastic technique, the bias correction and stochastic analog method (BCSA) to downscale daily GCM precipitation fields to reproduce the temporal statistics and spatial autocorrelation structure of observed daily precipitation fields. They applied the BCSA technique to downscale daily precipitation projections from four GCMs to a 12-km grid scale over the state of Florida and evaluated their method compared to an interpolation-based simple statistical downscaling method (i.e., bias correction and spatial disaggregation method, BCSD) (Wood *et al.*, 2002), a modified version of BCSD which reverses the orders of the procedure (i.e., spatially downscaled followed by bias correction, SDBC) (Abatzoglou and Brown, 2012), and the bias correction constructed analog method (Hidalgo *et al.*, 2008). They showed that the BCSA exhibited superior skills in reproducing both the spatial and temporal statistics of observed gridded daily precipitation over other methods that tended to underestimate spatial variability.

This study evaluates the relative ability of three statistical downscaling methods: (1) the BCSD method; (2) the SDBC method; and (3) the BCSA method, to downscale daily GCM precipitation outputs to irregular subbasin (~3 to ~300 km^2) resolution and to simulate hydrologic response over the Tampa Bay region (10,370 km^2) in west-central Florida using a physically based and spatially distributed hydrologic model. The downscaling methods were applied to four GCM retrospective precipitation simulations from 1961 to 2000. The skill of each method in reproducing temporal and spatial statistics of subbasin precipitation observations was evaluated using various indices (e.g., spatial and temporal statistics, transition probabilities, spatial correlation indices, and variograms). The retrospective temperature predictions from each GCM were bias corrected using a simple cumulative distribution function (CDF)-

mapping method that assumes direct correspondence between the GCM grid cell containing the temperature observation and the observation exceedence probabilities. The use of a simpler bias correction procedure for temperature is warranted because spatial variability in daily temperature is not as significant as for daily precipitation in this region. The downscaled precipitation and temperature datasets were used in an integrated surface-subsurface hydrologic model (integrated hydrologic model [IHM]) (Geurink and Basso, 2013) to evaluate their relative skills in reproducing retrospective streamflow statistics over the study area.

STUDY DOMAIN AND DATA

Tampa Bay Region: The Integrated Northern Tampa Bay Model

Tampa Bay Water, the largest water supply agency in west-central Florida, operates a diverse regional water supply system and manages surface and groundwater water sources in compliance with permitted withdrawal limits to protect the ecological integrity of rivers, wetlands, and lakes in the Tampa Bay region. In this region, the fresh groundwater flow system generally consists of a thin surficial aquifer underlain by the thick, highly productive carbonate rocks of the Floridan aquifer system. Most of the Floridan aquifer is semiconfined, recharged from the overlying surficial aquifer. However, in the northern extent of the region, some portions of the Floridan aquifer are unconfined, receiving direct recharge from vadose zone infiltration. The significant temporally variable flux and storage connection between surface water and groundwater systems are caused by the near-surface water table condition that covers more than 50% of the region.

To capture the dynamic interaction between surface water and groundwater in this region, the IHM was developed which integrates the EPA Hydrologic Simulation Program-Fortran (Bicknell *et al.*, 2001) for surface water modeling with the U.S. Geological Survey (USGS) MODFLOW96 (Harbaugh and McDonald, 1996) for groundwater modeling. IHM was designed to provide advanced simulation capability of the complex interactions of surface water and groundwater features in shallow water table environments. The model can be characterized as deterministic, semidistributed parameter, semiimplicit real-time formulation, with variable time steps and spatial discretization (Ross *et al.*, 2004). The model components explicitly account for all significant hydrologic processes including precipitation, interception, ET, runoff, recharge, streamflow, base flow, groundwater flow, and all the component storages of surface, vadose, and saturated zones (Ross *et al.*, 2005). Climate input data requirements include time series for precipitation and reference ET for each subbasin (Geurink *et al.*, 2006b).

To assist water supply planning and operations, Tampa Bay Water developed and calibrated the Integrated Northern Tampa Bay (INTB) model using the IHM (Geurink *et al.*, 2006a) simulation engine. The 10,370 km^2 INTB model domain (Figure 1) is bordered in the east by the Gulf of Mexico and in the west by an inland groundwater divide (Geurink and Basso, 2013). Tampa Bay is located in the southwest part of the domain. The north and east boundaries are modeled as steady-state no-flux boundaries that follow the Floridan aquifer divide, the southeast boundaries are modeled as general head boundaries defined using observed well data around this region, and the western offshore boundaries are modeled as constant head boundaries (Geurink *et al.*, 2006a; Geurink and Basso, 2013). All boundaries are located far from the area of interest for this study to minimize their influence on findings of the study.

The surface water component of the model domain is discretized into 172 subbasins (ranging in area from 3.4 to 362.7 km^2) based on surface drainage for hydrologic modeling as shown in Figure 1. For each subbasin, hydrologic processes are simulated within hydrologic response units (land segments) based on five upland land-use categories and two water-body categories (Ross *et al.*, 2004). Land cover over the domain is diverse, including urban, grassland, forest, agricultural, mined land, water, and wetlands. Open water and wetlands cover about 25% of the region.

GCM Archive

In this study, outputs from four GCM retrospective simulations: BCCR-BCM 2.0, CCSM, CGCM 3.1, and GFDL-CM 2.0 (hereafter BCCR, CCSM, CGCM, and GFDL, respectively) were obtained from the World Climate Research Programme's (WCRP's) Coupled Model Inter-comparison Project phase 3 (CMIP3) multimodel dataset for 1961-2000 (Table 1). The grid resolutions for the GCMs range from 1.4° to 2.8° and thus the entire study area is covered by at most four grids for each GCM. Figure 1 shows how each model grid configuration covers the study domain.

Meteorological Data

The spatiotemporal distribution and intensity of precipitation are important factors in deterministic,

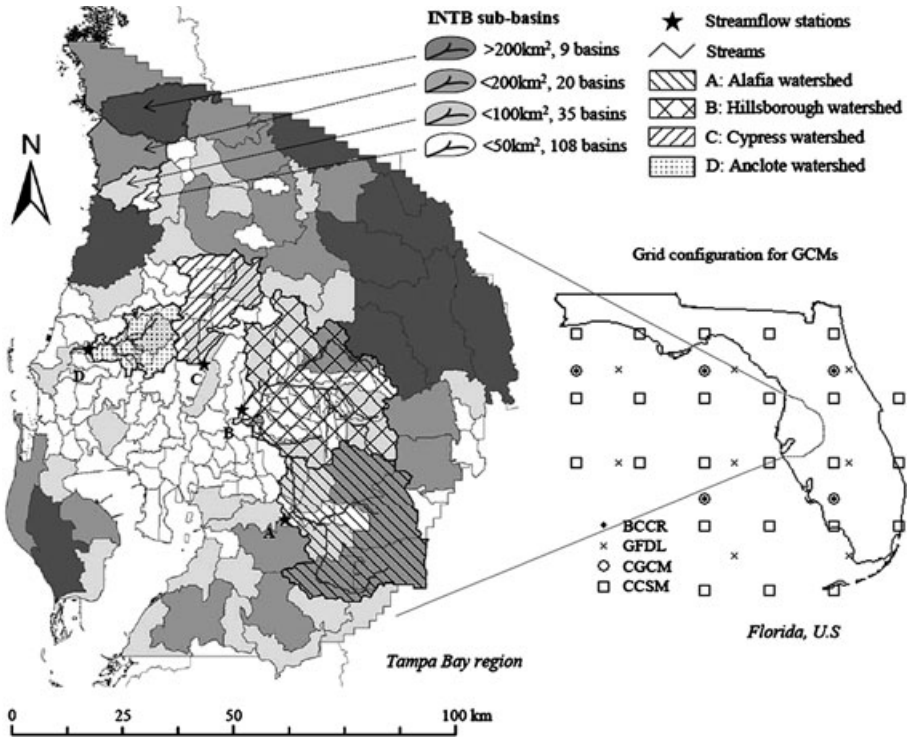

FIGURE 1. Map of Study Area, Subbasin Configuration (for Integrated Northern Tampa Bay [INTB] model domain), Grid Configuration of General Circulation Models (GCMs), and Target Stations for Streamflow Evaluation. See Table 1 for explanation of four GCMs.

TABLE 1. GCMs Used in This Study.

Modeling Group, Country	WCRP CMIP3 I.D.	Acronym	Grid Resolution	Primary Reference
Bjerknes Centre for Climate Research, Norway	BCCR-BCM2.0	BCCR	2.8° × 2.8°	Furevik *et al.* (2003)
U.S. Department of Commerce/NOAA/Geophysical Fluid Dynamics Laboratory, United States	GFDL-CM2.0	GFDL	2.0° × 2.5°	Delworth *et al.* (2006)
Canadian Centre for Climate Modeling & Analysis, Canada	CGCM3.1	CGCM	2.8° × 2.8°	Flato and Boer (2001)
National Center for Atmospheric Research, United States	CCSM3	CCSM	1.4° × 1.4°	Collins *et al.* (2006)

Note: GCM, general circulation model; WCRP CMIP3, World Climate Research Programme's Coupled Model Inter-comparison Project phase 3; NOAA, National Oceanic and Atmospheric Administration.

physically based hydrologic simulations. A high spatiotemporal resolution is required to adequately capture the effects of localized convective storms, a dominant type of precipitation event during the wet season in Florida (Rokicki, 2002). The INTB model requires 15-min precipitation time series for each of the 172 subbasins.

Observed precipitation data over the INTB model domain were obtained for 300 stations from three different sources including Tampa Bay Water, Southwest Florida Water Management District (SWFWMD), and National Oceanic and Atmospheric Administration (NOAA). Unfortunately 15-min precipitation data were only available at a few NOAA precipitation gages. Therefore, to estimate the subbasin precipitation time series for input to the hydrologic model, all available precipitation data within each basin were aggregated to a daily total then spatially distributed using Thiessen polygons over the 172 subbasins (Figure 1). Within the INTB model the daily precipitation values for each of the subbasins were temporally disaggregated using 15-min observations from the nearest NOAA station that matched the total rainfall of the day (i.e., a historical analog approach: Geurink and Basso, 2013). The same temporal disaggregation approach was applied to the statistically downscaled daily precipitation results.

The INTB model used minimum and maximum daily temperature data ($T_{\min}$ and $T_{\max}$) from six NOAA stations in the region to estimate reference ET using Hargreaves equation (Hargreaves and Samani, 1985). Reference ET time series were estimated using

TABLE 2. Target Stations for Streamflow Simulation.

Streamflow Stations	Watershed	Latitude	Longitude	Drainage Area (km^2)
Alafia River at Lithia	Alafia	27.8719	−82.2114	867.3
Hillsborough River near Zephyrhills	Hillsborough	28.1497	−82.2325	569.6
Cypress Creek at Worthington Gardens	Hillsborough	28.1856	−82.4008	302.9
Anclote River near Elfers	Anclote	28.2139	−82.6667	187.7

data from these six stations and then spatially assigned to the 172 subbasins within the model domain using a nearest-neighbor approach. Precipitation and temperature data from 1989 to 2006 were used for hydrologic model calibration and verification (Geurink and Basso, 2013). These data were also used in bias correction and downscaling of GCM results.

Hydrologic Data

Hydrologic observations from 1989 to 1998 and from 1999 to 2006 were used for the INTB model calibration and verification, respectively (Geurink and Basso, 2013). Hydrologic observations included 38 streamflow monitoring stations and 200 locations each of surficial and Floridan aquifer wells. Additional hydrologic data including pumping for irrigation and public water supply and surface water withdrawals for public water supply were collected from USGS, the SWFWMD, and Tampa Bay Water and used to develop the INTB model.

Four streamflow stations on the major rivers (Figure 1 and Table 2) were chosen to evaluate hydrologic response to the alternative downscaled climate predictions, based on their importance to water supply management and variability in flow characteristics over the study area. The river flows at these stations are important for water supply operations because they are either located near or downstream of well fields or water is withdrawn from them to meet local water demand. The Alafia and Hillsborough rivers have a mean discharge of 8.6 and 6.2 m^3/s, respectively, with very few no-flow days, whereas Cypress Creek and the Anclote River have a mean discharge of less than 2 m^3/s. Furthermore, Cypress Creek has a large percentage (approximately 20%) of no-flow days. Investigating stations with large and small flow volumes is important to understand how different types of flow regimes are affected by spatio-temporal differences in downscaled climate data.

METHODOLOGY

The statistical downscaling methods examined in this study are composed of two processes: bias correction and spatial disaggregation. While the technique for bias correction is the same in each case, the spatial disaggregation methods and order of the processes are different among the methods. For the BCSD and BCSA methods, bias correction is performed at the GCM grid scale before spatial disaggregation, requiring local observations to be aggregated up to the GCM scale. For the SDBC method bias correction is performed after spatial disaggregation to the subbasin scale, so subbasin observations are used directly. In the following section, the common bias correction technique is described. In the subsequent sections, the particular data, disaggregation method, and order of processes are detailed for each of the three statistical downscaling methods. Figure 2 provides a schematic representation for each of the methodologies.

Bias Correction of Climate Data

A CDF mapping approach (Panofsky and Brier, 1968; Wood *et al.*, 2002; Ines and Hansen, 2006) was used to bias correct the raw GCM outputs (for the BCSD and BCSA methods) or downscaled raw GCM outputs (for the SDBC method). CDF mapping is the most common method for bias correction of climate model outputs (Wood *et al.*, 2004). The method effectively removes the bias in the temporal statistics (including mean, variance, skewness, kurtosis, etc.) of precipitation and temperature predictions by adjusting the simulated CDF to fit the observed CDF (Hwang *et al.*, 2011, 2013).

The procedure for bias correction used in this study is described as follows: (1) CDFs of observed daily precipitation data including the zero precipitation days were created individually for each calendar month at the appropriate spatial resolution for bias correction, i.e., GCM grid cell (for BCSD and BCSA) or subbasin (for SDBC). These 12 monthly CDFs were used for bias correction of the daily outputs. (2) CDFs of GCM simulated daily precipitation were created for each calendar month at the appropriate spatial resolution (GCM grid cell for BCSD and BCSA, subbasin for SDBC). (3) Daily outputs were bias corrected at the appropriate resolution using CDF mapping that preserves the probability of exceedence of the simulated precipitation, but corrects the precipi-

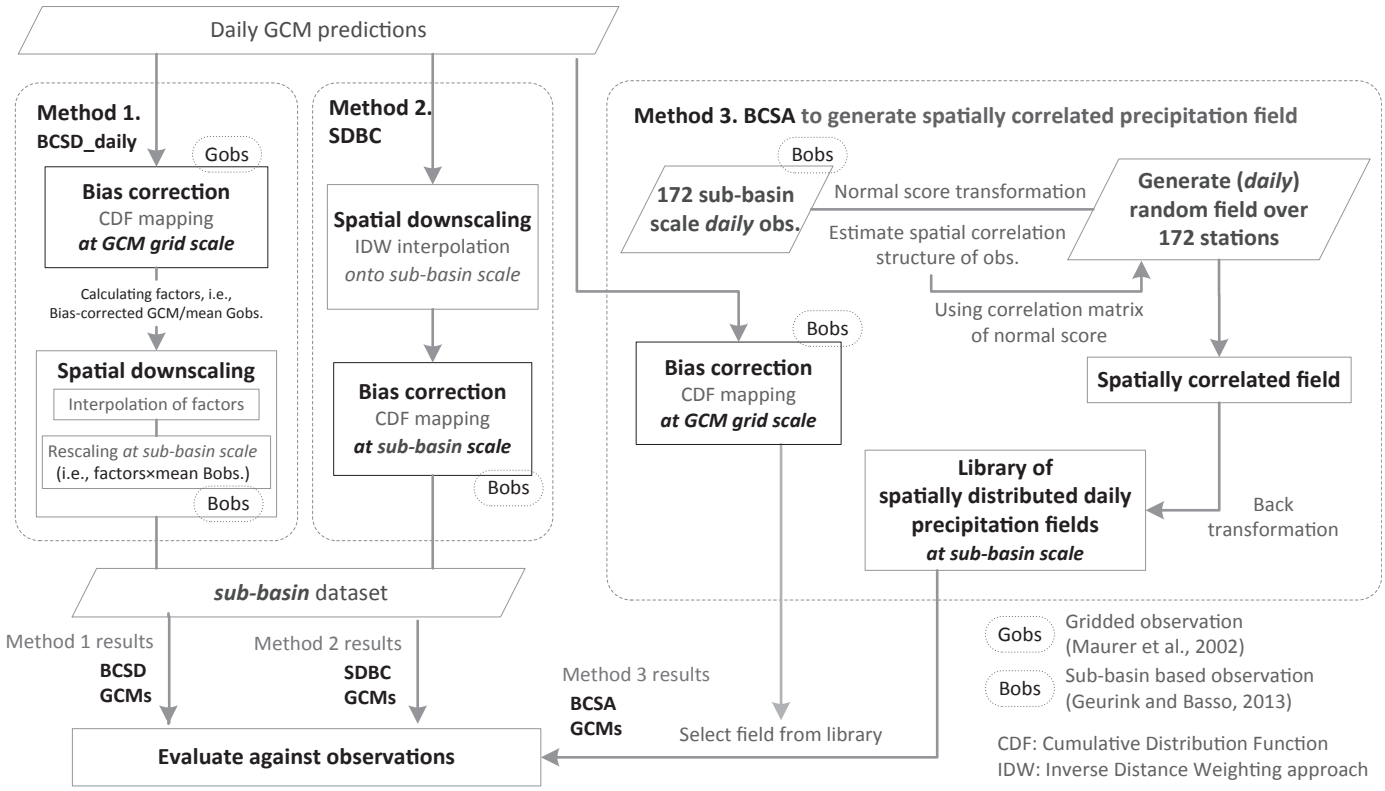

FIGURE 2. Schematic Representation of the Methodology for Bias Correction and Spatial Disaggregation at Daily Time Scale (BCSD_daily), Spatial Disaggregation and Bias Correction (SDBC), and Bias Correction and Stochastic Analog Method (BCSA) Downscaling Techniques. In each case, the entire process is conducted independently for each calendar month using daily general circulation model (GCM) and observed data.

tation to the value that corresponds to the same probability of exceedence from the observed CDFs. Thus, bias-corrected rainfall $x'_{t,i}$ on day t at grid or subbasin i was calculated as,

$$x'_{t,i} = F^{-1}_{\mathrm{obs,i}}\left(F_{\mathrm{sim,i}}(x_{t,i})\right) \quad (1)$$

where $F(\cdot)$ and $F^{-1}(\cdot)$ denote a CDF of daily precipitation x and its inverse, and subscripts "sim" and "obs" indicate downscaled simulation and observed daily rainfall, respectively. Because CDFs were developed from all data including the zero precipitation days, Equation (1) preserves the probability of rain events as well as the temporal statistics (i.e., mean, variance, skewness, kurtosis, etc.) that the observed daily data exhibit. However, it should be noted that although the method removes biases for the particular time scale at which bias correction is conducted (e.g., daily scale in this study), it does not guarantee improvement in the timing of precipitation events or the magnitude of precipitation events accumulated to different time scales.

Statistical Downscaling Methods

BCSD_daily Method. The BCSD method is an empirical statistical technique developed by Wood *et al.* (2002) to downscale GCM products. Although there is disagreement as to whether the simple interpolation method should be categorized as a statistical downscaling method (Schmidli *et al.*, 2006), the BCSD method was classified as a statistical downscaling method for this study because it bridges the coarse resolution GCM outputs and the fine resolution climate inputs required for impact assessment models (Wood *et al.*, 2004; Iizumi *et al.*, 2011). Whereas the BCSD method has conventionally been used to downscale climate data at monthly scales (Wood *et al.*, 2004; Maurer *et al.*, 2010), in this study the method was extended to downscale daily GCM results. We refer to this approach as "BCSD_daily" hereafter in this article.

The BCSD_daily method consists of two separate steps: bias correction followed by spatial downscaling. Details of the procedure are depicted schematically in

Figure 2 and enumerated as follows. (1) Gridded daily precipitation observations from Maurer *et al.* (2002) were aggregated up to the raw GCM scale and monthly CDFs for the aggregated daily observed data were constructed for each GCM grid cell over Florida; (2) monthly CDFs of GCM simulated daily precipitation were created for each GCM grid cell; (3) daily GCM simulations were bias corrected using the CDF mapping approach described above; (4) coarse-scale factors (i.e., bias-corrected GCM precipitation/aggregated observed mean daily precipitation for the appropriate month) were spatially interpolated from the GCM grid cells over the state of Florida to the subbasin centroids using an inverse distance weighting (IDW) approach (Shepard, 1984); (5) interpolated subbasin factors were rescaled using the mean daily precipitation at the subbasin scale calculated using subbasin-based observations for the appropriate month.

Although gridded observations were used for initial bias correction (because the interpolation process included some GCM grid cells outside the model domain where subbasin observations were not available), subbasin-based observations were used to rescale the interpolated factors at the subbasin scale (i.e., in step 5) to reproduce the mean precipitation of subbasin observations used to calibrate the model.

SDBC Method. Recently, Abatzoglou and Brown (2012) modified the BCSD method by changing the order of the BCSD procedures to improve the BCSD method results at the daily time scale. The SDBC method applied in this study generally follows the procedure developed by Abatzoglou and Brown (2012), except the monthly CDFs were developed using daily precipitation data for each calendar month instead of using a 15-day moving window centered on each calendar day for CDF mapping. Details of the procedure, as modified for this study, are enumerated as follows: (1) coarse-scale daily GCM precipitation outputs were interpolated to the subbasin centroids using an IDW approach; (2) monthly CDFs of observed daily precipitation were created for each subbasin in the model domain; (3) monthly CDFs of interpolated GCM daily precipitation were created for each subbasin in the model domain; (4) daily GCM simulations for each subbasin were bias corrected using the CDF mapping approach described above.

BCSA Method. The BCSA method was developed by Hwang and Graham (2013) to downscale daily GCM results to produce fine-scale daily precipitation outputs which preserve both the temporal statistical characteristics as well as the spatial correlation structure of observed precipitation fields. This method can downscale daily GCM precipitation outputs to any spatial configuration or resolution (e.g., point, grid, or subbasin) where the temporal statistics and spatial correlation among observations can be estimated. The method uses the observed temporal and spatial statistics among the spatially distributed observations to generate synthetic precipitation fields which honor the observed statistics.

The first step in the BCSA procedure is to generate an ensemble of synthetic precipitation fields that honor the observed spatiotemporal statistics. The procedure was conducted separately for each month because the spatiotemporal statistics for daily rainfall (e.g., temporal CDF, spatial correlation structure, etc.) vary over the year. Details of the procedures are as follows: (1) for each subbasin the observed daily precipitation data for that month were transformed into standard normal variables using a normal score transformation approach (Goovaerts, 1997); (2) correlation coefficients between the normal score transform variables were estimated for all pairs of subbasin daily precipitation data; (3) an ensemble of synthetic spatially correlated random daily precipitation totals, that preserve the estimated correlations for that month, was generated over the subbasins using the Cholesky decomposition method (Taussky and Todd, 2006); (4) the synthetic normal score transform fields were back-transformed to the original observed distributions at each subbasin. An ensemble of 3,000 realizations of precipitation for each month was produced for this study.

Next, the daily raw GCM precipitation data were bias corrected using the spatially aggregated subbasin-based observation over each corresponding GCM grid cell. Finally, for each day that the coarse-scale bias-corrected GCM results predicted nonzero rainfall a realization from the appropriate monthly ensemble was selected for which the spatial mean of the generated precipitation field most closely matched the coarse-scale bias-corrected GCM result. Any difference between the spatial mean precipitation of the best-fit-generated precipitation field and the coarse-scale bias-corrected GCM precipitation (generally <0.1 mm) was removed by multiplying the generated field by a scaling factor (i.e., spatial mean of bias-corrected GCM field/spatial mean of precipitation field chosen from the ensemble). An ensemble size of 3,000 was chosen because it produced a detailed enough set of realizations so that a realization with an areal rainfall volume within 0.1 mm of the GCM prediction could always be found. Inclusion of more realizations within the ensemble did not significantly improve the match. For days that the coarse-scale bias-corrected GCM results predicted zero rainfall over the domain, each subbasin was assigned zero rainfall.

Hydrologic Modeling

Geurink and Basso (2013) calibrated the IHM model from 1989 to 1998 and verified its performance from 1999 to 2006 (18-year total period) using the observed data described above to produce the INTB application. In this study the observed precipitation and temperature data used in the calibrated INTB model were replaced by the downscaled GCM daily precipitation and temperature datasets developed in this study. For each downscaled GCM, the INTB model simulation was run using precipitation and temperature for two consecutive 18-year periods extracted from the 40-year retrospective period (i.e., the 36-year period from 1965 to 2000). All other parameters, forcing terms, initial conditions, and boundary conditions were identical to those used in the calibrated INTB model to focus on differences created by the downscaled temperature and precipitation data.

RESULTS AND DISCUSSION

Statistically Downscaled GCM Results

Temperature. Figure 3 compares the mean daily T_{min} and T_{max} from each of the raw GCMs (spatially averaged over the study area using the area weighting method) to the observed mean daily T_{min} and T_{max} (averaged over the six stations) for each month of the year. The observed mean daily T_{max} ranged from 22.0°C (in January) to 32.8°C (in August) and the observed mean daily T_{min} ranged from 10.4°C (in January) to 23.1°C (in August). The spatial variability in mean T_{min} and T_{max} observations over the six stations is represented by error bars on the figure. These plots indicate that the range of the observed mean T_{max} over the six stations was higher (i.e., 1.6-2.2°C, ≈3% of the mean T_{max}) during the winter and spring than the summer (i.e., 0.9-1.5°C, ≈8% of the mean T_{max}). Observed mean T_{min} was, in general, more spatially variable than observed mean T_{max} (i.e., 3.5°C, ≈20% of mean T_{min}) over the entire annual cycle.

All of the raw GCMs showed errors in the magnitude of T_{min} and T_{max} (typically underestimating both) as well as the pattern of the monthly cycle of T_{max} (e.g., GCM peaks occurring in March through June instead of July and August) and the monthly cycle of T_{min} (GCM peaks occurring in May through June for T_{min} instead of July and August). After bias correction, however, all the GCM results exactly follow the magnitude and timing of the observed mean temporal cycle for both T_{min} and T_{max} since the temperature data are bias corrected on a daily basis using observed monthly CDFs.

Precipitation. Figure 4 shows the temporal mean and standard deviation of daily precipitation for the observations and raw GCM predictions averaged over the domain for each month of year. The spatial variation in the observed mean daily precipitation over the 172 subbasins is shown in Figure 4a and the spatial variation in the observed standard deviation of daily precipitation is shown in Figure 4b. The range of the mean daily precipitation over the 172 subbasins varied from 0.7 mm in November (46%

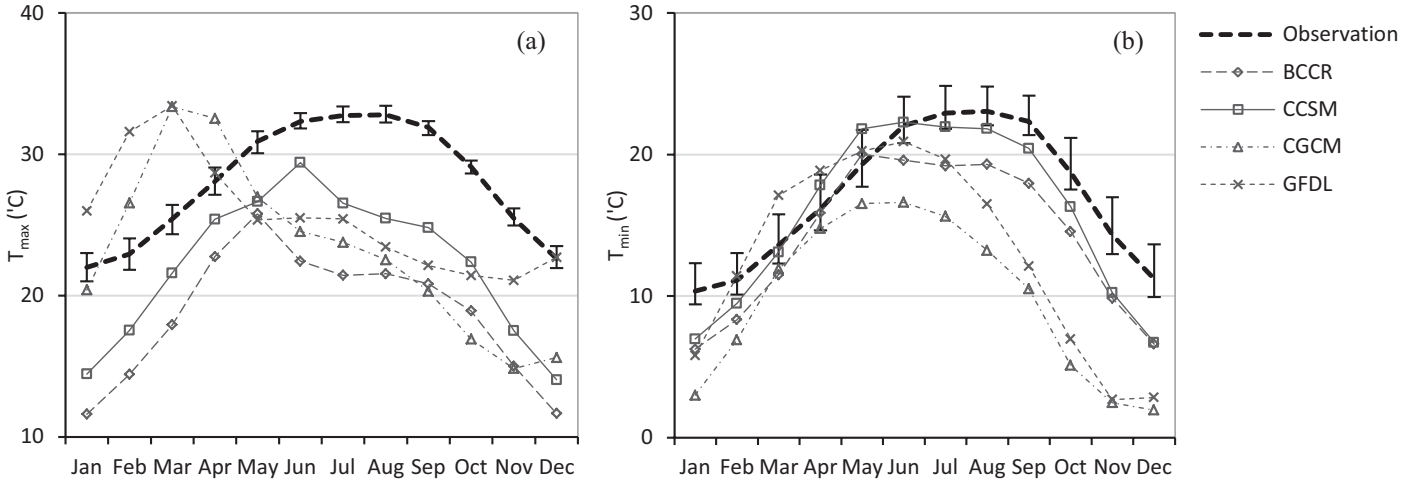

FIGURE 3. Mean Daily T_{max} and T_{min} of Basin-Based Observations and Raw General Circulation Model (GCM) Results by Month. Mean daily temperatures for the bias corrected GCMs are identical to observed. Error bars on the graphs represent the range of T_{max} and T_{min} average over six point locations. See Table 1 for explanation of four GCMs.

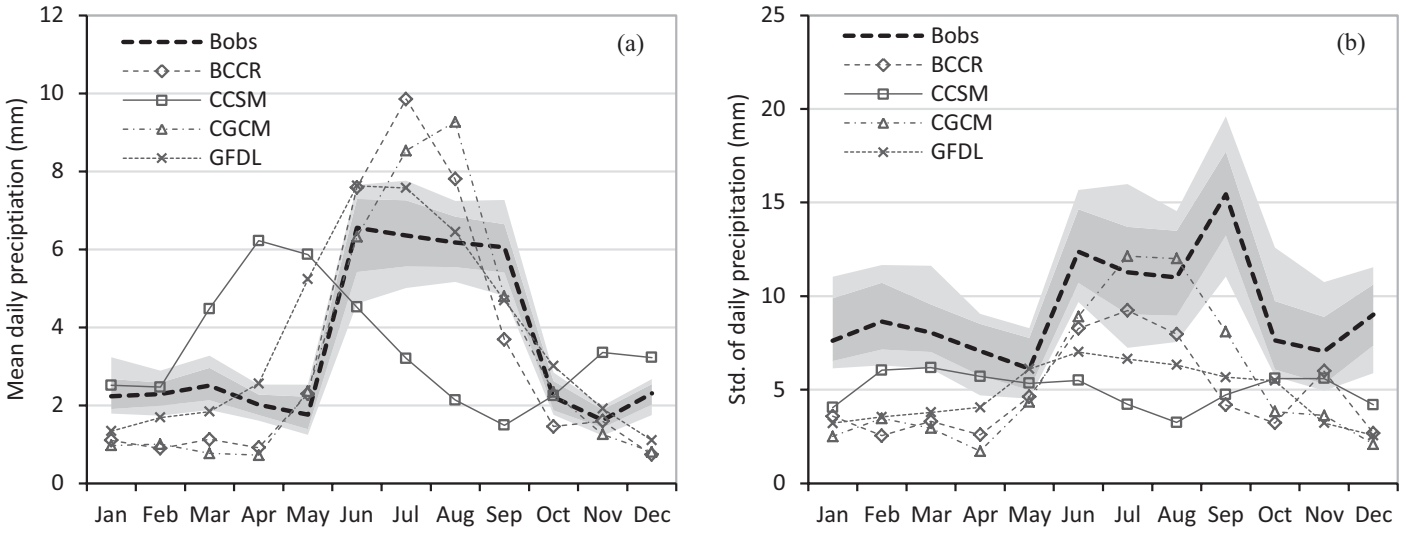

FIGURE 4. (a) Mean Daily Precipitation and (b) Standard Deviations (Std.) of Daily Precipitation for Basin-Based Observations (Bobs, 1988-2006) and Raw General Circulation Model (GCM) Outputs by Month Averaged over the Domain. The bright and dark gray zones represent total data range and 5-95th percentile for Bobs, respectively, reflecting spatial variation in the mean (a) and Std. (b) of daily precipitation over the 172 subbasins. Note that bias-corrected GCM results exactly reproduce observed mean and std. of daily precipitation. See Table 1 for explanation of four GCMs.

of spatially averaged observations) to 2.9 mm in June (45% of spatially averaged observations) which is significantly greater than the spatial variability that was exhibited by the temperature data.

The raw GCM precipitation results indicate that while BCCR, CGCM, and GFDL overestimated wet season precipitation (June through August), these raw GCM predictions generally reproduced the observed seasonal pattern of highest rainfall during the summer. On the other hand, the raw CCSM results did not reproduce the observed seasonal pattern of rainfall for the region, predicting highest rainfall in March and April which are among the driest months, and lowest rainfall in August and September which are typically among the wettest months. Furthermore, all the GCM results tended to underestimate the temporal standard deviation of daily precipitation (Figure 4b) with average monthly error between observed and GCM standard deviation of daily precipitation ranging from −3.8 mm or −41% (CGCM) to −4.5 mm or −48% (BCCR).

Bias correction using the CDF mapping approach on a daily basis forces the reproduction of the temporal mean of daily precipitation observations, thus all the downscaling methods used in this study match the observed mean daily precipitation cycle over the subbasins exactly (thus statistically downscaled results for mean daily precipitation are not shown). However, the skill in reproducing the standard deviation of daily precipitation varies among the downscaling methods. Figure 5 compares average temporal standard deviation of the downscaled daily GCM precipitation to the average temporal standard deviation of observed daily precipitation over the 172 subbasins for each month. The figure shows that whereas SDBC

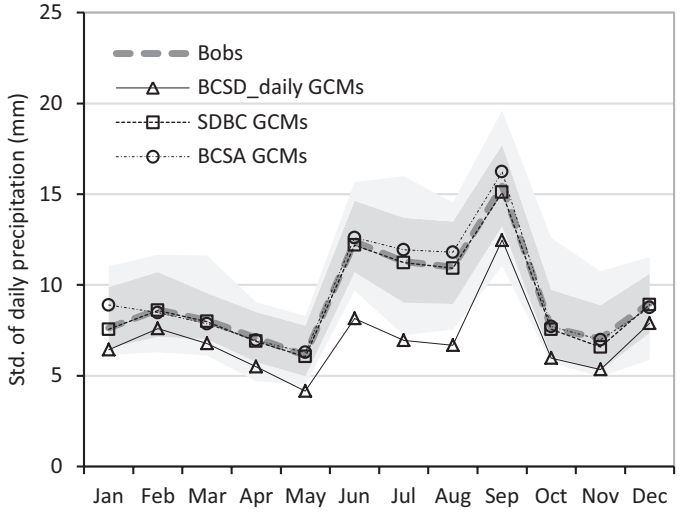

FIGURE 5. Standard Deviations (Std.) of Daily Precipitation for Basin-Based Observations (Bobs), Bias Correction and Spatial Disaggregation at Daily Time Scale (BCSD_daily), Spatial Disaggregation and Bias Correction (SDBC), and Bias Correction and Stochastic Analog Method (BCSA) General Circulation Models (GCMs) for Each Month Averaged over the Domain. The differences among the four GCM results are negligible (<0.1 mm, ≈1%) and thus the average over the GCMs is presented here. The bright and dark gray zones represent total data range and 5-95th percentile of standard deviation of Bobs, respectively, reflecting spatial variation in the Std. over the 172 subbasins. Note that all downscaling methods match the observed average daily precipitation cycle shown in Figure 4a exactly.

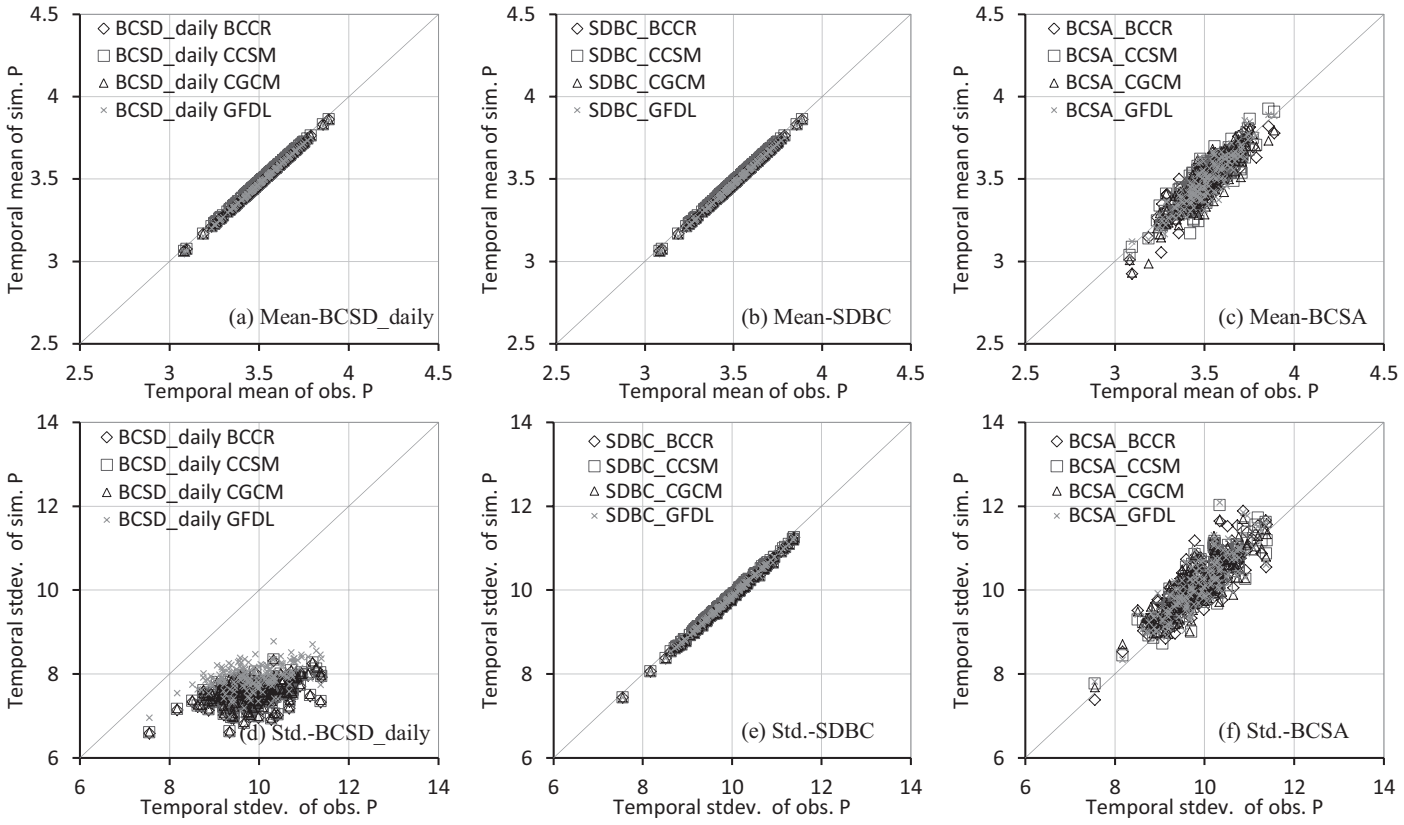

FIGURE 6. Scatter Plots of Temporal Mean (a-c) and Standard Deviation (d-f) of Observed and Downscaled 172 Basin-Based Daily Precipitation Data Using Bias Correction and Spatial Disaggregation at Daily Time Scale (BCSD_daily) (first column), Spatial Disaggregation and Bias Correction (SDBC) (second column), and Bias Correction and Stochastic Analog Method (BCSA) (third column). See Table 1 for explanation of four GCMs.

and BCSA successfully reproduce the observed temporal standard deviation of daily precipitation, the BCSD_daily method underestimates the temporal standard deviation of daily precipitation by 12-39%, with more significant underestimation during the wet season from June to September. This result is due to the temporally smoothed time series created by the interpolation of bias-corrected precipitation from the coarse GCM resolution to the subbasin scale. Iizumi *et al.* (2011) found similar results and concluded that simple statistical downscaling methods may be inaccurate for reproducing temporal variation patterns, and less physically plausible because of oversimplification of the underlying local-scale physical processes. Note that individual GCMs are not separately represented in Figure 5 because differences among the four GCM results (i.e., standard deviation of daily precipitation) for a given downscaling technique are negligible (<0.1 mm, ≈1%).

Figure 6 compares temporal means and standard deviations of the daily precipitation results using the three downscaling methods over the entire data period for each of the 172 subbasins individually. The BCSD_daily method estimates the temporal mean accurately for all subbasins, but underestimates the temporal standard deviation of daily rainfall by 8-32% for all subbasins. The SDBC method accurately estimates both the mean and the standard deviation of daily rainfall for all subbasins. The BCSA method reproduces the mean and standard deviation of daily precipitation patterns in general; however, the errors for individual subbasins are larger than for the SDBC method. The BCSA ensemble is generated randomly from the observed CDF; thus, differences between the mean generated from the ensemble and from the data are due to sampling from a limited number of replicates (3,000 in this study). This could possibly be improved by increasing the size of ensemble or improving the accuracy of the random field generator in the BCSA process.

While the SDBC method most accurately reproduces temporal statistics of daily precipitation at each station, the method overestimates the temporal standard deviation of spatially averaged daily precipitation over the domain, as shown in Figure 7. This figure indicates that the BCSD_daily and BCSA accurately reproduced the standard deviation of average precipitation over the study area. However, the

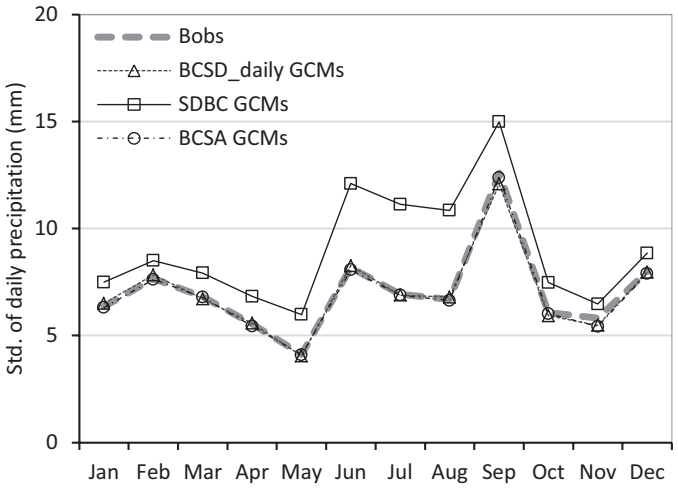

FIGURE 7. Standard Deviation (Std.) of Spatially Averaged Daily Precipitation over the Domain for Basin-Based Observations (Bobs), Bias Correction and Spatial Disaggregation at Daily Time Scale (BCSD_daily), Spatial Disaggregation and Bias Correction (SDBC), and Bias Correction and Stochastic Analog Method (BCSA) General Circulation Models (GCMs) for Each Month. The differences among the four GCM results were negligible and thus the average Std. over the GCMs is presented here.

SDBC process resulted in significant overestimation of the temporal standard deviation of spatially averaged precipitation, even though it showed good skill in reproducing temporal standard deviation of daily precipitation for each basin individually (Figures 5 and 6). This is due to the fact that in the SDBC procedure the daily GCM precipitation predictions are spatially disaggregated by interpolation and then bias correction at the downscaled grid resolution. Thus, the probability of exceedence of the daily precipitation generated at the coarse GCM grid scale is reproduced at each local grid cell, exaggerating the spatial extent of the effects of extreme events, particularly in the summer wet season which is dominated by small-scale convective thunderstorms.

In addition to the temporal mean and standard deviation of daily precipitation, day-to-day precipitation patterns are important for most hydrologic applications. For instance, the occurrence of consecutive wet and dry days reflects dynamic properties of precipitation that have important implications for producing extreme hydrologic behavior (i.e., flood and drought events). Hence, daily transitions between wet and dry states were calculated using the first-order transition probability (Haan, 1977) for the observed data, the raw and bias-corrected GCM data, and the downscaled bias-corrected GCM data (Figure 8). These results indicate that the raw GCM outputs significantly overestimated the dry-to-wet (P01) and wet-to-wet (P11) transition probabilities compared to observations in both the wet and dry seasons. Note that raw GCM results predict areally averaged precipitation over a large area, and thus may be expected to include more wet days than observations at finer scales because a wet day occurs if precipitation falls anywhere in the large grid cell.

The bias-corrected GCM scale results for the grid nearest to the study area showed considerable improvement in reproducing the fine scale observed P01 in the dry season, but showed little improvement in reproducing P11 in the dry season, P01 in the wet season, or P11 in the wet season. Similar to the raw and bias-corrected GCM results, the BCSD_daily results significantly overestimated P01 and P11 transition probabilities because direct interpolation of bias-corrected coarse-scale GCM results creates more rainy days with small precipitation events at the subbasin scale than exhibited by the observations. In contrast, transition probabilities produced using SDBC and BCSA results matched observed transition probabilities quite well for both seasons, with higher transition probabilities (both P01 and P11) in the wet season. Note that the observed spatial variation in wet-to-wet transition probability over the 172 subbasins is larger than dry-to-wet transition probability for both seasons and this observed spatial variance is accurately reproduced by the BCSA method.

Spatial variability in daily precipitation was examined by calculating the number of rainy subbasins as a function of spatially averaged precipitation for both the wet and dry seasons (Figure 9). This figure indicates that the number of subbasins predicted to be rainy (defined as >0.1 mm for a subbasin) differs significantly among the three downscaling methods. The interpolation-based spatial downscaling methods (i.e., BCSD_daily and SDBC) tend to overestimate spatial correlation, and thus simulate an excessive number of rainy subbasins, except for the large precipitation events (>10 mm). The BCSD_daily results showed the most serious overprediction of the number of rainy subbasins with more than 50% of study domain estimated to be rainy in the wet season even for small precipitation events (<0.1 mm, spatially averaged precipitation). The SDBC method showed improvement over the BCSD_daily method, but still simulated too many rainy subbasins for both seasons. On the other hand, the BCSA method successfully reproduced the number of rainy subbasins for both seasons.

While the number of rainy basins with respect to the magnitude of precipitation events is one indicator of the spatial correlation of daily rainfall, the relationship between the geographical distance and correlation are not conveyed by this measure. We used the variogram, defined as the expected value of the squared difference of the values of the random field separated by certain distance (Goovaerts, 1997), to

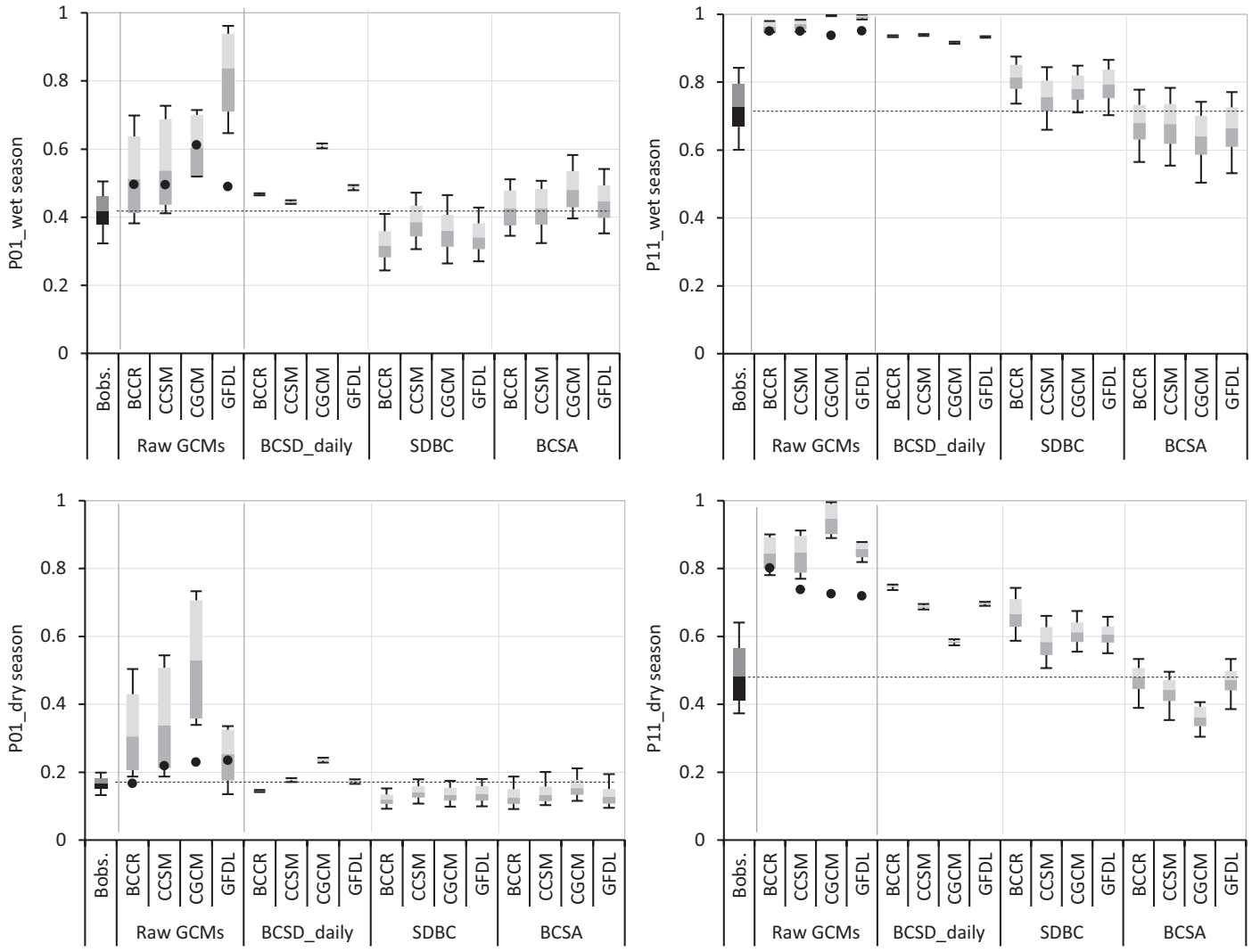

FIGURE 8. Comparison of Transition Probabilities (i.e., dry-to-wet day [P01, left column] and wet-to-wet day [P11, right column]) of Subbasin Observations (Bobs.), Raw General Circulation Models (GCMs), Bias Correction and Spatial Disaggregation at Daily Time Scale (BCSD_daily), Spatial Disaggregation and Bias Correction (SDBC) Results, and Bias Correction and Stochastic Analog Method (BCSA) Results for Wet (top) and Dry Season (bottom). Box plots represent the minimum, 10th percentile, 90th percentile, and maximum transition probability over the study area indicating spatial variation in the transition probabilities. The black dots on the raw GCM results are the transition probabilities of bias-corrected GCM results (at the GCM scale) for the grid nearest to the study area. The dashed lines indicate the mean of Bobs. transition probabilities. See Table 1 for explanation of four GCMs.

evaluate how well each downscaling technique reproduces the spatial correlation structure of the observed daily precipitation. Variograms were estimated for daily observations and the downscaled daily GCM precipitation results for both the wet and dry seasons. Figure 10 compares the estimated variograms among the three downscaling methods to the observed variogram. These figures indicate that the BCSD_daily and SDBC results significantly underestimated the observed variogram at all separation distances, but that the BCSA reproduced the observed variograms accurately for both wet (June through September) and dry (October through May) seasons. Note that differences among the variograms for individual GCM results were not significant compared to differences among the downscaling methods.

Hydrologic Simulation Results

The calibrated INTB model was run to simulate streamflows using the statistically downscaled climate datasets. The monthly pattern of mean daily streamflow is commonly used to evaluate hydrologic implications of climate predictions (e.g., Wood *et al.*, 2004; Dibike and Coulibaly, 2005). Figure 11 compares mean daily streamflow, by month, predicted using the climate input data (i.e., precipitation and

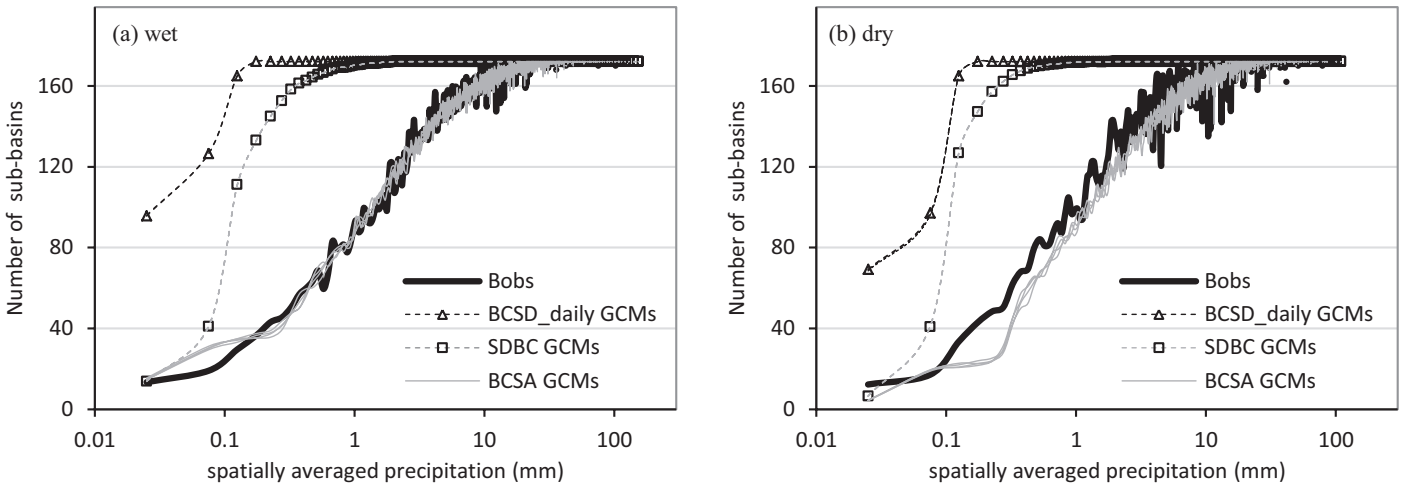

FIGURE 9. Comparison of Number of Rainy Subbasins as a Function of Spatially Averaged Precipitation for (a) Wet and (b) Dry Season. Observation (Bobs) were compared to the results of three different downscaling methods.

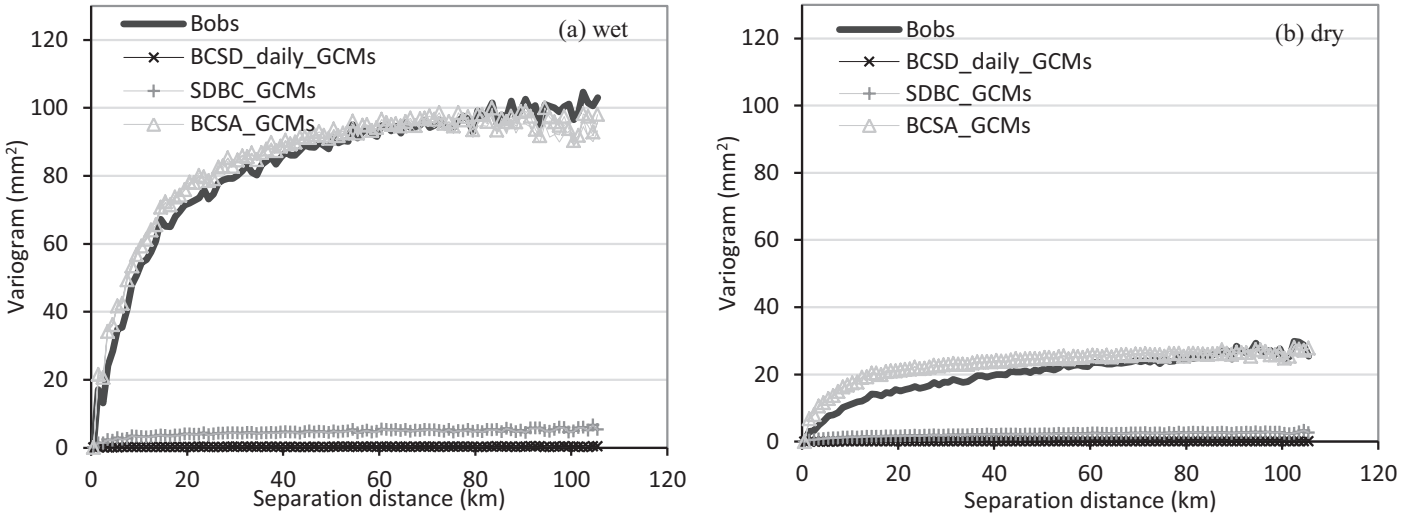

FIGURE 10. Comparison of Variograms of Subbasin-Based Observations (Bobs) and the Downscaled Predictions Using Bias Correction and Spatial Disaggregation at Daily Time Scale (BCSD_daily), Spatial Disaggregation and Bias Correction (SDBC), and Bias Correction and Stochastic Analog Method (BCSA) Techniques for (a) Wet and (b) Dry Season.

temperature) from the various downscaling methods to INTB calibrated model results and observations for the four target stations. Note that comparing the simulated results to the calibrated results evaluates differences due only to variations in climatic forcing, whereas comparing to observations reflects both climatic forcing and hydrologic modeling errors.

Results indicate that for all downscaling techniques the monthly pattern of mean daily streamflow was similar to observed and calibrated results during the dry season from October through May. However, all methods tended to underestimate the streamflow during the early portion of the wet season from June through August. The BCSD_daily method underestimated streamflow in the wet season more significantly than the SDBC and BCSA methods at all stations (Table 3). This is due to the highly spatially correlated small precipitation events produced by the BCSD_daily method (Figures 9 and 10) that result in overestimation of ET over the domain. Figure 12 compares the total annual ET estimated over the domain for each climate input and the calibrated model. These results show that the BCSD_daily results overestimated the total ET by 3.1-5.3% over the model domain. Note that the temporal distribution of daily reference ET estimated using the different downscaled climate inputs was identical for each station because the temporal distributions of daily

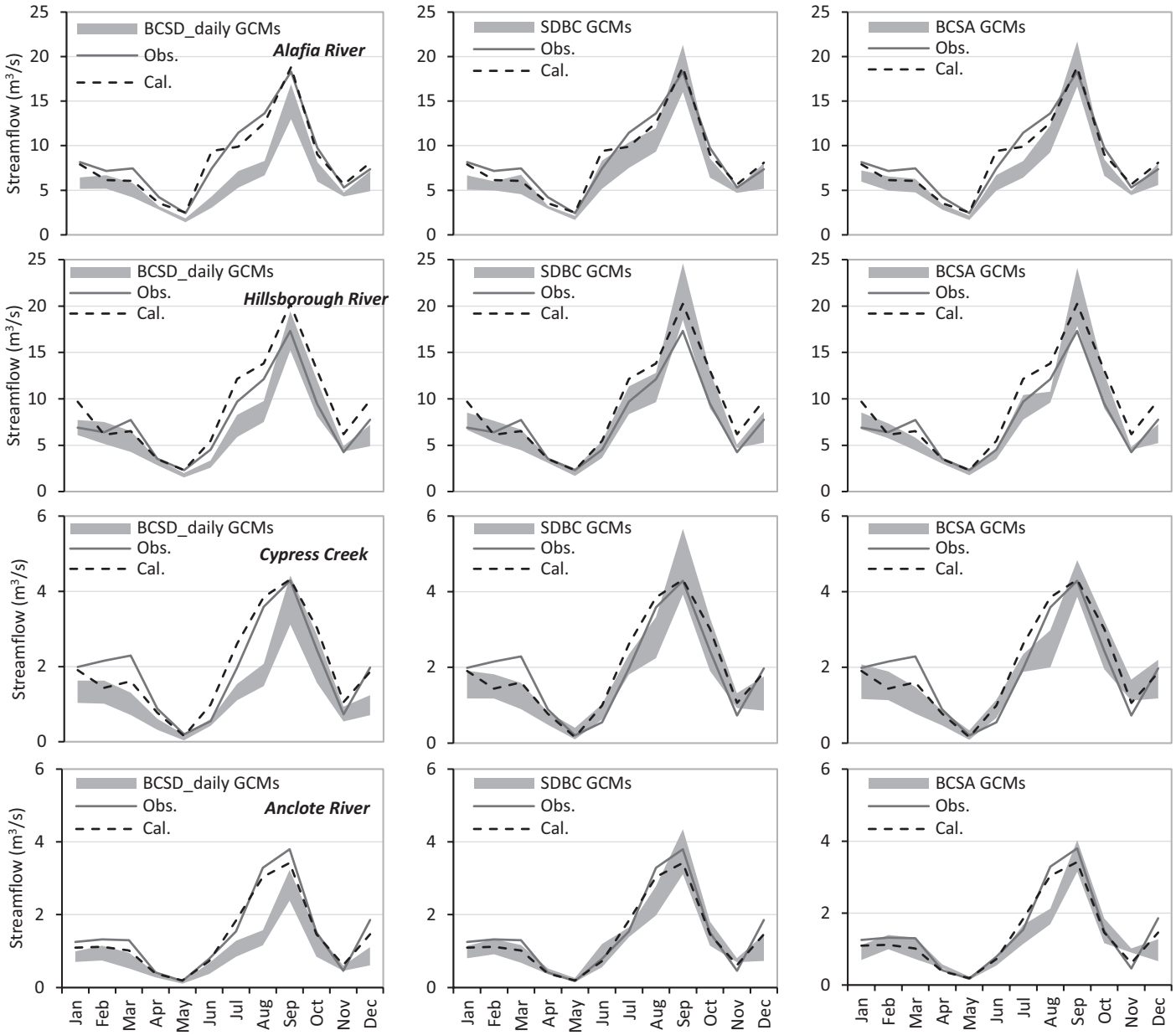

FIGURE 11. Comparison of Mean Daily Streamflow Predicted by Month Using Downscaled Climate Scenarios Produced by Bias Correction and Spatial Disaggregation at Daily Time Scale (BCSD_daily) (first column), Spatial Disaggregation and Bias Correction (SDBC) (second column), and Bias Correction and Stochastic Analog Method (BCSA) (third column) to the Calibrated Results (Cal.) and Observations (Obs.). The gray zones represent the range of simulation results for the four general circulation models (GCMs).

temperature at each station were exactly matched to the observed distribution through the bias correction process.

Figure 13 compares the standard deviation of daily streamflow predicted using each of the methods to the observed and calibrated results. This figure indicates that the SDBC results significantly overestimated the temporal standard deviation of daily streamflow during the wet season from June to September, especially for the larger subbasins (Alafia River and Hillsborough River, see also Table 3). This is due to the fact that SDBC overpredicts the spatial correlation of large precipitation events during the wet season (see Figures 7, 9, 10) which leads to overprediction of high streamflow events, especially for larger subbasins that integrate rainfall over larger areas.

The averaged mean differences (i.e., simulated-calibrated) and errors (i.e., simulated-observed) of the temporal mean and standard deviation of daily streamflow simulation over the four GCMs for the wet and dry seasons are compared in Table 3. The

TABLE 3. Average Mean Error (simulated-observed) and Average Mean Differences (simulated-calibrated) of the Temporal Mean and Standard Deviation of Daily Streamflow for Wet and Dry Season over the Four General Circulation Models.

Average Mean Error (simulated-observed)

Unit: m^3/s		Temporal Mean of Daily Streamflow				Temporal Standard Deviation of Daily Streamflow			
Downscaling Methods		**Calibrated**	**BCSD_daily**	**SDBC**	**BCSA**	**Calibrated**	**BCSD_daily**	**SDBC**	**BCSA**
Wet season	Alafia	−0.038	**−4.633**	−1.550	−2.264	3.534	−3.431	**7.622**	1.312
	Hillsborough	2.003	**−2.199**	0.504	−0.075	0.176	−2.352	**3.880**	−1.209
	Cypress Creek	0.345	**−0.836**	−0.101	−0.168	−0.773	**−1.914**	−0.577	−1.380
	Anclote	−0.100	**−0.943**	−0.268	−0.480	−1.967	**−2.636**	−0.637	−1.631
	Avg. error	*0.553*	***−2.153***	*−0.354*	*−0.747*	*0.243*	*−2.572*	***2.583***	*−0.727*
Dry season	Alafia	−0.037	**−2.092**	−1.280	−1.333	0.918	**−1.609**	0.225	−0.728
	Hillsborough	0.912	**−0.926**	−0.194	−0.465	0.798	−2.715	−1.354	**−3.235**
	Cypress Creek	−0.071	**−0.568**	−0.289	−0.226	−0.749	**−0.957**	−0.480	−0.475
	Anclote	−0.118	**−0.404**	−0.175	−0.194	−0.704	**−0.615**	0.036	−0.095
	Avg. error	*0.172*	***−0.998***	*−0.485*	*−0.555*	*0.066*	***−1.474***	*−0.393*	*−1.133*

Average Mean Differences (simulated-calibrated)

Unit: m^3/s		Temporal Mean of Daily Streamflow			Temporal Standard Deviation of Daily Streamflow		
Downscaling Methods		**BCSD_daily**	**SDBC**	**BCSA**	**BCSD_daily**	**SDBC**	**BCSA**
Wet season	Alafia	**−4.595**	−1.513	−2.226	−4.401	**4.089**	−2.222
	Hillsborough	**−4.201**	−1.499	−2.078	−2.528	**3.703**	−1.386
	Cypress Creek	**−1.181**	−0.445	−0.513	**−1.141**	0.196	−0.607
	Anclote	**−0.843**	−0.169	−0.381	−0.669	**1.330**	0.337
	Avg. difference	***−2.705***	*−0.907*	*−1.300*	*−2.185*	***2.330***	*−0.970*
Dry season	Alafia	**−2.055**	−1.243	−1.296	**−2.143**	−0.309	−1.262
	Hillsborough	**−1.839**	−1.106	−1.377	**−3.602**	−2.242	−3.123
	Cypress Creek	**−0.496**	−0.217	−0.155	**−0.878**	−0.402	−0.396
	Anclote	**−0.286**	−0.056	−0.076	**−0.537**	0.114	−0.017
	Avg. difference	***−1.169***	*−0.656*	*−0.726*	***−1.790***	*−0.710*	*−1.200*

Notes: Bold indicates the largest error or difference among the methods. Italic indicates the average error or difference over the streamflow stations for each season.

BCSD_daily, bias correction and spatial disaggregation at daily time scale; SDBC, spatial disaggregation and bias correction; BCSA, bias correction and stochastic analog method.

results confirm that the SDBC and BCSA methods predict mean streamflow with better accuracy than the BCSD_daily method. For example, for the SDBC and BCSA results averaged errors over the stations were approximately -0.4 m^3/s (~13% of observed mean streamflow) and -0.7 m^3/s (~17% of observed mean streamflow), respectively, for the wet season. However, the averaged error of the BCSD_daily results was -2.2 m^3/s (~39% of observed mean streamflow) for the wet season. The statistics in the table also confirm that the BCSD_daily method underestimates the temporal standard deviation of daily streamflow throughout the year for all stations, whereas the SDBC method overestimates the temporal standard deviation of daily streamflow in the wet season for the large stations. The BCSA method produces the lowest average error in temporal standard deviation in the wet season and comparable errors to the SDBC method in the dry season.

The statistical significance of the differences between the observed and simulated mean monthly streamflows over the study period was examined by month and by target station using the two-sample *t*-test. The cases for which the calibrated model and downscaled GCMs predicted mean monthly streamflows that were not statistically significantly different from observed mean monthly streamflows at significance level $p = 0.05$ are shown in Table 4. The mean monthly streamflows predicted by the calibrated model were found to be statistically equal to the observed mean monthly streamflows for 33 of a total of 48 possible cases (i.e., 4 stations × 12 months). The results for the downscaled GCM simulations varied by month and station, however, the BCSD_daily results showed the fewest cases from which mean monthly streamflows was found to be statistically equal to observed mean monthly streamflow at the 0.05 significance level, i.e., 19% of the 192 total cases

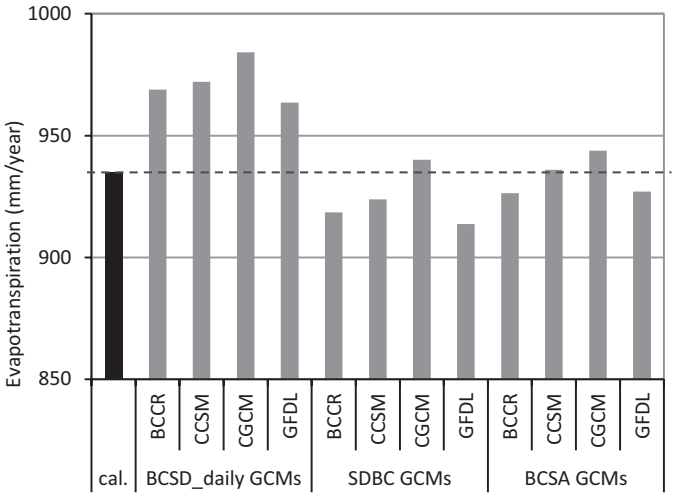

FIGURE 12. Comparison of Simulated Mean Annual Evapotranspiration over the Integrated Northern Tampa Bay Model Domain. cal. indicates the results using observed climate input data. See Table 1 for explanation of four GCMs.

(i.e., 12 months × 4 stations × 4 GCMs). In particular for the wet season, few BCSD_daily cases (e.g., only BCCR results for the Anclote River in June and none of the GCMs for any of the rivers in July and August) were found to have acceptable skill in reproducing mean streamflow. The SDBC and BCSA methods showed improvement over the BCSD method, with 34% of all cases for SDBC and 33% of all cases for BCSA showing mean monthly predictions that showed no statistical difference from the observed results at the 0.05 significance level.

In addition to accurate predictions of the mean and standard deviation of daily streamflow, accurately predicting the magnitude and frequency of extreme flow events is critical for water management. Figure 14 compares the annual frequency of daily streamflow events as a function of the daily streamflow. Results indicate that for streamflows up to the 95th percentile (indicated in the Figure 14 for each station) the frequency of daily streamflow events was accurately reproduced by all methods. However, for all downscaling methods the magnitude of low-frequency, extremely high daily streamflow tended to exceed the magnitude of observed extreme daily streamflow events. Of the three downscaling methods, the SDBC method overestimated the frequency of high streamflow events most significantly. As discussed previously, the SDBC method overestimated the temporal standard deviation of spatially averaged precipitation and daily streamflow predictions (Figures 7 and 13) because the large-scale daily GCM precipitation simulations are bias corrected at the downscaled grid resolution at the last step in the procedure. Thus, on a daily basis the rainfall for each downscaled subbasin preserves the precipitation percentile event predicted by the large-scale GCM, exaggerating the spatial extent of high percentile events.

To evaluate predictions of the duration of high streamflow events, the 7Q10 and 7Q2 high streamflows were calculated for each downscaling method and compared to the observed and calibrated results (Figure 15). Note that the 7Q10 (7Q2) high flow is the annual seven-day maximum streamflow that is expected to occur on average in one of 10 (2) years. 7Q10 and 7Q2 low flows (i.e., seven-day minimum streamflow) are also important indices in terms of water quality and supply management. However, 7Q10 and 7Q2 low flow for the target stations are quite small, i.e., less than 1 m^3/s even for high streamflow stations (i.e., Alafia River and Hillsborough River stations) and differences among the downscaling methods and calibrated results were not significant and thus are not shown here.

Figure 15 shows that SDBC tended to overestimate the 7Q10 high flows compared to the calibrated results especially for large subbasins (i.e., average percent difference over all the GCMs of 27% [41 m^3/s] for the Alafia River, 12% [12 m^3/s] for the Hillsborough River, <1% [<1 m^3/s] for the Cypress Creek, and 14% [4 m^3/s] for Anclote River). The BCSD_daily and BCSA 7Q10 results showed lower errors in estimated 7Q10 for all stations (i.e., average percent error from −11 to 5%). The SDBC results also overestimated the 7Q2 high flows compared to calibrated results (i.e., by an average of 26% [13 m^3/s] for Alafia River, 3% [2 m^3/s] for Hillsborough River, 30% [3 m^3/s] for Cypress Creek, and 43% [4 m^3/s] for Anclote River). The BCSD_daily results, in contrast, underestimated 7Q2 for all subbasins by an average of −17% (−9 m^3/s) for Alafia River, −32% (−17 m^3/s) for the Hillsborough River, −15% (−1 m^3/s) for Cypress Creek, and −17% (−2 m^3/s) for Anclote River. The BCSA 7Q2 results, on average, showed the best fit to those estimated from the observations with averaged errors from −5% (Cypress Creek) to 14% (Anclote River). Note that the greater error ratios for 7Q2, especially for the small basins, are due to the small magnitude of the 7Q2 flows in these watersheds.

While the different GCMs showed differences in estimates of both 7Q10 and 7Q2, the ranges over the downscaled GCM results using BCSA were in general smallest (45%, percent ratio of the 7Q10 ranges among GCMs compared to calibrated results (i.e., 7Q10 range of GCMs/calibrated 7Q10, on average over the stations)) compared to the others (58 and 70% for BCSD_daily and SDBC, respectively). Note that the variation among the GCMs that derive from differences in temporal regimes produced by the raw GCM results are not removed through the bias correction conducted in this study.

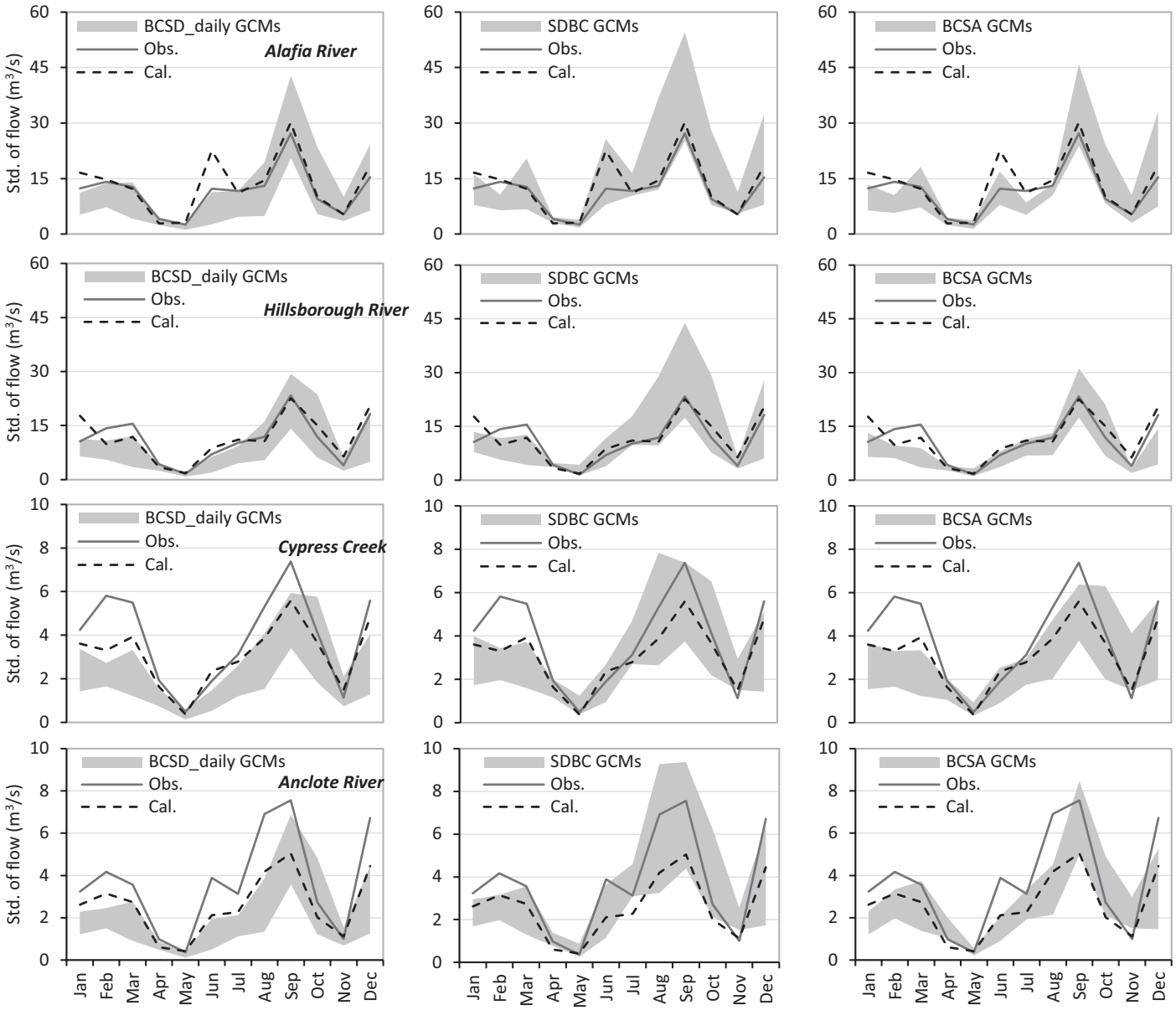

FIGURE 13. Comparison of Standard Deviation (Std.) of Daily Streamflow Predicted by Month Using Downscaled Climate Scenarios Produced by Bias Correction and Spatial Disaggregation at Daily Time Scale (BCSD_daily) (first column), Spatial Disaggregation and Bias Correction (SDBC) (second column), and Bias Correction and Stochastic Analog Method (BCSA) (third column) to the Calibrated Results (Cal.) and Observations (Obs.). The gray zones represent the range of simulation results for four general circulation models (GCMs).

SUMMARY AND CONCLUSIONS

This study compared the relative ability of three different statistical downscaling techniques to reproduce retrospective subbasin scale spatiotemporal precipitation characteristics, and to predict retrospective streamflow statistics when used to drive a physically based spatially distributed hydrologic model in the Tampa Bay region of west-central Florida. Four GCMs were chosen to examine the skills of statistical downscaling methods. While the retrospective precipitation predictions were downscaled using three different statistical downscaling methods, the retrospective temperature predictions from GCMs were downscaled using the same CDF mapping bias correction method that assumes direct correspondence between the exceedence probabilities of GCM grid cell and observation location for all cases.

Results indicated that the temporal mean of $T_{\min}$ and $T_{\max}$ were well reproduced by bias correction-based downscaling. Similarly, all downscaled precipitation results accurately reproduced the temporal mean of daily precipitation over all subbasins. How-

TABLE 4. Results of the Two-Sample *t*-Test for the Statistical Significance of the Difference between the Observed and Simulated Mean Monthly Streamflows. *Indicates that calibrated mean streamflow for the indicated station and month were not statistically significantly different from the observed mean streamflow at $p = 0.05$. Similarly, letters in the table (i.e., A: BCCR, B: CCSM, C: CGCM, D: GFDL) indicate that mean streamflow using the indicated GCM and downscaling technique were statistically equal to the observed mean streamflow at $p = 0.05$. See Table 1 for explanation of four GCMs.

		***vs.* Observed Daily Streamflow**			
Month	**Watershed**	**Calibrated**	**BCSD_daily**	**SDBC**	**BCSA**
January	Alafia	*			D
	Hillsborough		A, C	A, C	A, C
	Cypress Creek	*		B	B
	Anclote	*	D	B, D	D
February	Alafia	*	A, D	D	D
	Hillsborough	*	A, B, D	A, B, C	A, B, C, D
	Cypress Creek				
	Anclote	*	D	D	A, B, D
March	Alafia	*		A	A
	Hillsborough	*		A	
	Cypress Creek				
	Anclote	*		A, D	A, D
April	Alafia				
	Hillsborough	*	A	A, B, D	A, B, D
	Cypress Creek			A	A
	Anclote	*	A	B, C	C
May	Alafia	*			
	Hillsborough	*		A	A
	Cypress Creek		A	C	D
	Anclote	*	A	B	C, D
June	Alafia	*		A, B	A
	Hillsborough	*		B, D	A, B
	Cypress Creek	*		A, B, C	A, B, D
	Anclote	*	A	B, C	A, B, D
July	Alafia			A	
	Hillsborough			C	A, C
	Cypress Creek	*			A
	Anclote	*		B, C, D	A, C, D
August	Alafia	*		D	
	Hillsborough				D
	Cypress Creek	*		D	D
	Anclote				D
September	Alafia	*	A, B	A, B, D	B, C, D
	Hillsborough		A, B, D	C, D	D
	Cypress Creek	*	A	B, D	A
	Anclote	*		A, B, D	A, B, D
October	Alafia	*		D	D
	Hillsborough		C	A, C	A
	Cypress Creek	*	B, D	B	
	Anclote	*	B, D	B, C	B, C
November	Alafia	*	A	A, D	D
	Hillsborough		C		D
	Cypress Creek		A, D		
	Anclote		A, B, C		
December	Alafia	*	A, B	A, B, D	A, B, D
	Hillsborough	*	A, B, D	A, B, D	A, B
	Cypress Creek	*		B	B
	Anclote	*		B	

Note: BCSD_daily, bias correction and spatial disaggregation at daily time scale; SDBC, spatial disaggregation and bias correction; BCSA, bias correction and stochastic analog method.

ever, the accuracy in reproducing temporal variability, spatial variability, and spatial correlation structure of precipitation varied among the downscaling methods.

The BCSD_daily results underestimated temporal variability in daily rainfall and overestimated the wet-to-wet and dry-to-wet transition probabilities because the method produced unrealistic highly spa-

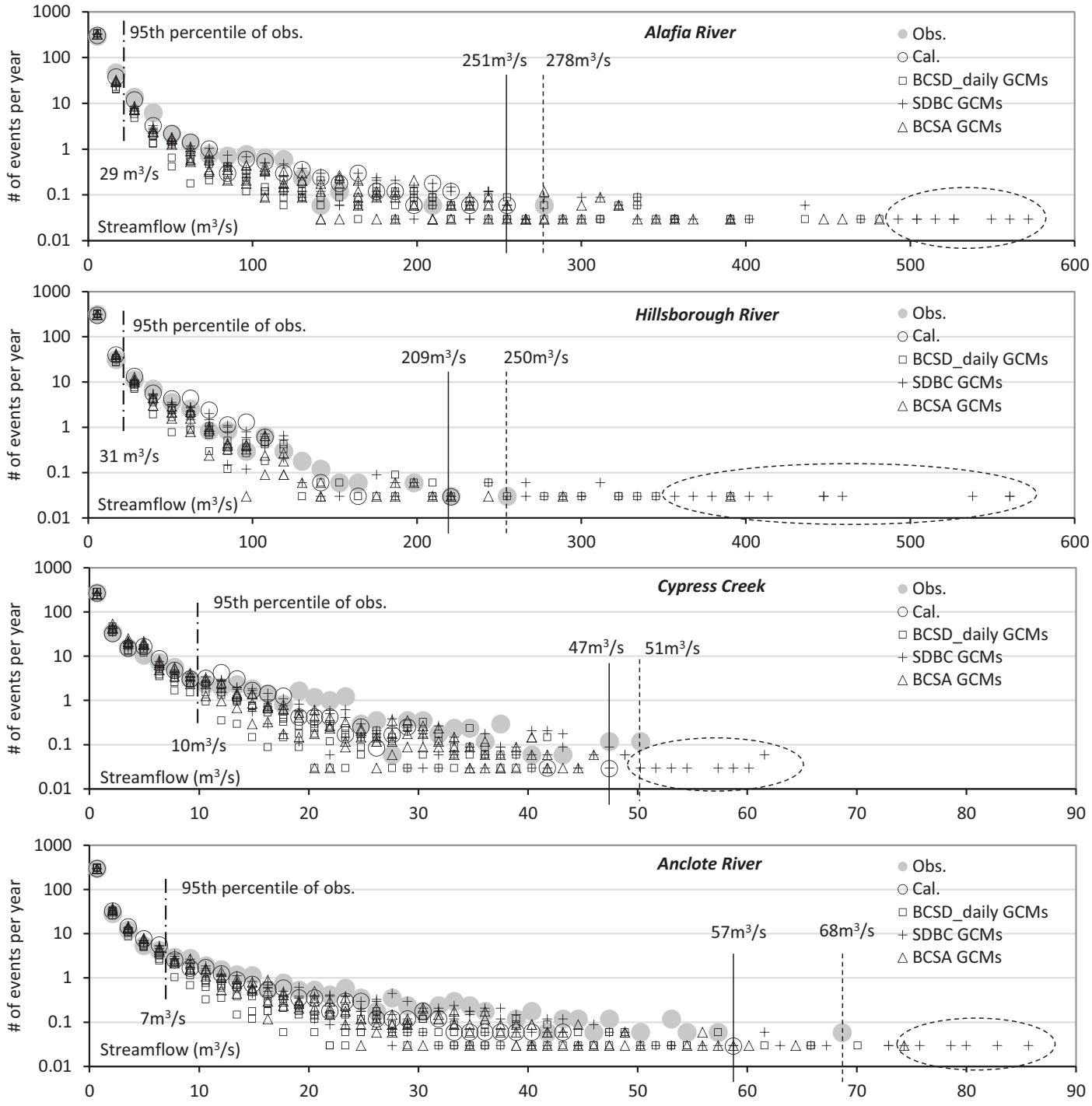

FIGURE 14. Comparison of Frequency of Observed (Obs.), Calibrated (Cal.), and Simulated Daily Streamflow Events per Year for Each Target Station. The dash dot lines indicate the 95th percentile of observed daily streamflow for each station, the solid and dashed lines indicate the maximum daily streamflow of calibrated results and observations, respectively, and dotted circles indicate the notable extreme events simulated by the spatial disaggregation and bias correction (SDBC) results. Differences among the results for each general circulation model (GCM) are negligible and thus GCMs were not presented separately.

tially correlated low-volume precipitation fields. The SDBC method improved over the BCSD_daily results in reproducing temporal variability in daily rainfall and daily transition probabilities by bias correcting at the downscaled grid resolution rather than at the coarse GCM resolution. However, SDBC tended to overestimate the temporal variability in spatially averaged precipitation due to the bias correction of

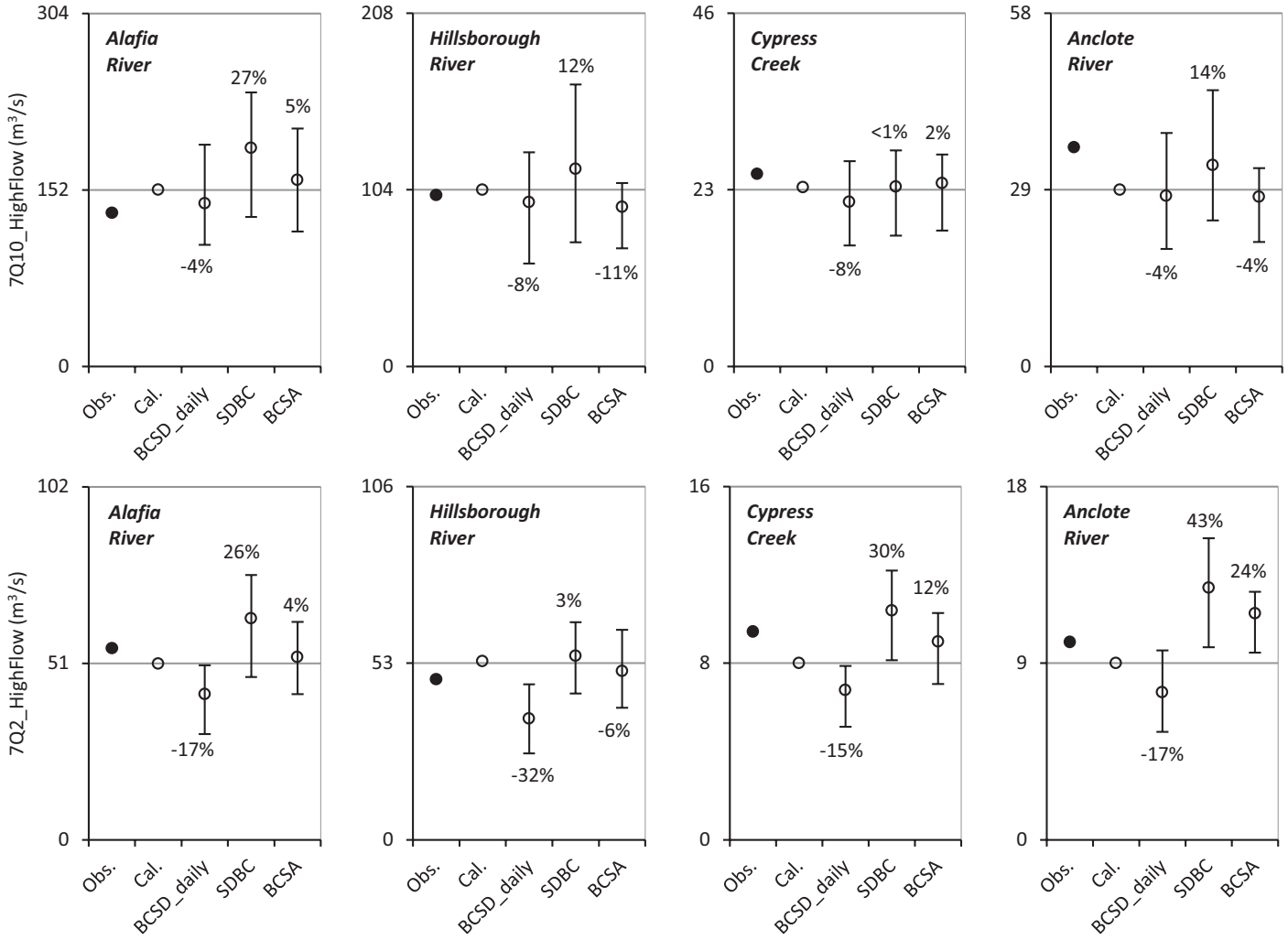

FIGURE 15. Comparison of the 7Q10_High Flow (top row) and 7Q2_High Flow (bottom row) Estimated from Observation (Obs.), Calibrated Results (Cal.), and Streamflow Simulations Using Three Different Downscaled General Circulation Model (GCM) Results (i.e., using BCSD_daily, SDBC, and BCSA). Open circles for downscaled results indicate the average values over the GCMs and error bars represent the range of the GCMs. The percent differences in averaged simulated value compared to the calibrated value are presented on each error bar.

smooth spatially interpolated GCM results at the subbasin scale. The BCSA reproduced the observed daily temporal precipitation variability and transition probabilities more accurately than the BCSD_daily and SDBC methods.

In terms of spatial variability in precipitation, significant differences between the interpolation-based downscaling methods and the new BCSA method were demonstrated. Overall, BCSD_daily failed to reproduce the observed spatial variability and produced overcorrelated precipitation fields. SDBC showed better skill in reproducing spatial variability compared to BCSD_daily but was still found to overestimate spatial correlation. The BCSA successfully reproduced the spatial variability exhibited by observations.

The differences among statistical downscaling techniques propagated into considerable differences in streamflow simulation results. The BCSD_daily method tended to underestimate monthly average streamflow for both wet and dry seasons at all target stations, due to overprediction of low-volume precipitation over large areas and thus overprediction of ET losses. The SDBC produced accurate mean streamflow estimates, however, overestimated the temporal standard deviation of daily streamflow in the wet season and overpredicted the magnitude of high streamflow events (7Q10, 7Q2, and peak daily streamflow). Thus, for the SDBC method under/overestimation of daily streamflow events apparently canceled out to produce approximately correct mean daily streamflow predictions. The BCSA method

showed comparable accuracy to the SDBC method in predicting mean streamflow, and reproduced the wet season standard deviation of daily streamflow and the magnitude of high streamflow events more accurately than the SDBC method. In all the precipitation and streamflow measures used in the study, the differences among statistical downscaling methods were more significant than the differences among GCMs.

It should be recalled that, through the bias correction process used in all methods, the daily CDF for precipitation was corrected to be identical to that of observed precipitation, and as a result mean daily precipitation over the study period was virtually identical for all downscaling methods. However, the results of the streamflow analyses indicate that, due to the nonlinear and integrative properties of the hydrologic system, reproducing more detailed precipitation characteristics (i.e., interevent duration, frequency of spatially averaged precipitation, daily precipitation spatial correlation structure) is required to accurately capture even the mean daily streamflow.

Accurately simulating both the spatial and temporal variability in precipitation inputs is important when assessing hydrologic implications of alternative climate scenarios in large, low-relief rainfall-dominated watersheds such as the Tampa Bay region in west-central Florida. Results of this study demonstrate that for this region simple interpolation-based statistical downscaling methods, such as BCSD_daily and SDBC that do not reproduce the spatial correlation structure of daily rainfall were not able to accurately reproduce higher order streamflow statistics such as the standard deviation of daily streamflow or the frequency of high streamflow events. Thus, for low-relief, rainfall-dominated watersheds where spatial variability in daily precipitation is high, the BCSA method is recommended for use over the BCSD_daily or SDBC methods. It should be noted that BCSA can be applied to downscale coarse resolution climate data (including other atmospheric variables such as, temperature) into any temporal (e.g., subdaily, monthly) and spatial scale (e.g., gridded or irregularly distributed points) needed for a particular application, as long as observations are available to estimate the CDFs and spatial correlation structure of the climate variable (Hwang and Graham, 2013).

Nevertheless, limitations of BCSA need to be carefully considered before applying the method in other applications. The spatial disaggregation process in BCSA is conducted independently on a daily basis, not taking into account characteristics of observed temporal sequence at the local scale. Thus, the skills in temporal trends and persistence of downscaled results rely on the skill of the large-scale bias-corrected GCMs. That is, if GCMs exhibit unrealistic temporal sequences of precipitation these limitations can propagate through the BCSA downscaling procedure into hydrologic predictions (see, for example, the magnitude of BCSA errors in Figures 8 and 15). These limitations could possibly be reduced by employing alternative bias correction methods developed to replicate observed temporal autocorrelation and thus interannual variability at multiple time scales (Johnson and Sharma, 2012; Mehrotra and Sharma, 2012) or by stochastically redistributing the temporal structure of climate model output (Ines *et al.*, 2011).

Furthermore, BCSA is conducted independently for each GCM grid and does not consider large-scale spatial correlation. Thus, use of BCSA for large areas covered by many GCM grids may produce discontinuities in local spatial correlation structure at the GCM grid boundaries. If application over large domains is required then the procedure could be revised as follows: (1) generate a library of spatially correlated precipitation fields at the local scale over the entire (multi-GCM grid) scale of interest, (2) choose the realization member that most closely matches the spatially averaged precipitation calculated over all the GCM grids, (3) scale the local precipitation field realizations within each individual GCM grid to match the GCM data of that grid cell.

The impacts of these BCSA limitations will vary from region to region, depending on climatic, topographic, geologic, and hydrologic characteristics. Therefore, it may be important to conduct similar quantitative hydrologic modeling experiments using alternative downscaling techniques to determine the most appropriate technique for other regions and applications of interest.

ACKNOWLEDGMENTS

This work is funded in part by the Sectoral Applications Research Program (SARP) of the NOAA Climate Program Office and by Tampa Bay Water. We also acknowledge the Program for Climate Model Diagnosis and Intercomparison (PCMDI) and the WCRP's Working Group on Coupled Modelling (WGCM) for their roles in making available the WCRP CMIP3 multimodel dataset. Support of this dataset is provided by the Office of Science, U.S. Department of Energy.

LITERATURE CITED

Abatzoglou, T.J. and J.T. Brown, 2012. A Comparison of Statistical Downscaling Methods Suited for Wildfire Applications. International Journal of Climatology 32:772-780.

Andréasson, J., S. Bergström, B. Carlsson, L.P. Graham, and G. Lindström, 2004. Hydrological Change-Climate Change Impact Simulations for Sweden. Journal of Human Environment 33:228-234.

Beven, K.J. and G.M. Hornberger, 1982. Assessing the Effect of Spatial Patterns of Rainfall in Modeling Stream Flow Hydrographs. Water Resources Bulletin 18(5):823-829.

Bicknell, B., J.C. Imhoff, J.L. Kittle, Jr., T.H. Jobes, and A.D. Donigian, Jr., 2001. Hydrologic Simulation Program-FORTRAN (HSPF): User's Manual for Version 12. U.S. Environmental Protection Agency, Athens, Georgia.

Busuioc, A., D. Chen, and C. Hellstrom, 2001. Performance of Statistical Downscaling Models in GCM Validation and Regional Climate Change Estimates: Application for SWEDISH Precipitation. International Journal of Climatology 21:557-578.

Cañón, J., F. Domínguez, and J.B. Valdés, 2011. Downscaling Climate Variability Associated with Quasi-Periodic Climate Signals: A New Statistical Approach Using MSSA. Journal of Hydrology 398:65-75.

Charles, S.P., B.C. Bates, I.N. Smith, and J.P. Hughes, 2004. Statistical Downscaling of Daily Precipitation from Observed and Modelled Atmospheric Fields. Hydrological Processes 18:1373-1394, doi: 10.1002/hyp.1418.

Christensen, J.H. and O.B. Christensen, 2003. Severe Summertime Flooding in Europe. Nature 421:805-806.

Collins, W.D., C.M. Bitz, M.L. Blackmon, G.B. Bonan, C.S. Bretherton, J.A. Carton, P. Chang, S.C. Doney, J.J. Hack, T.B. Henderson, J.T. Kiehl, W.G. Large, D.S. McKenna, B.D. Santer, and R.D. Smith, 2006. The Community Climate System Model Version 3 (CCSM3). Journal of Climate 19:2122-2143.

Delworth, T.L., A.J. Broccoli, A. Rosati, R.J. Stouffer, V. Balaji, J.A. Beesley, W.F. Cooke, K.W. Dixon, J. Dunne, K.A. Dunne, J.W. Durachta, K.L. Findell, P. Ginoux, A. Gnanadesikan, C.T. Gordon, S.M. Griffies, R. Gudgel, M.J. Harrison, I.M. Held, R.S. Hemler, L.W. Horowitz, S.A. Klein, T.R. Knutson, P.J. Kushner, A.R. Langenhorst, H.-C. Lee, S.-J. Lin, J. Lu, S.L. Malyshev, P.C.D. Milly, V. Ramaswamy, J. Russell, M.D. Schwarzkopf, E. Shevliakova, J.J. Sirutis, M.J. Spelman, W.F. Stern, M. Winton, A.T. Wittenberg, B. Wyman, F. Zeng, and R. Zhang, 2006. GFDL's CM2 Global Coupled Climate Models Part 1: Formulation and Simulation Characteristics. Journal of Climate 19:643-674.

Diaz-Nieto, J. and R.L. Wilby, 2005. A Comparison of Statistical Downscaling and Climate Change Factor Methods: Impacts on Lowflows in the River Thames, United Kingdom. Climatic Change 69:245-268.

Dibike, Y.B. and P. Coulibaly, 2005. Hydrologic Impact of Climate Change in the Saguenay Watershed: Comparison of Downscaling Methods and Hydrologic Models. Journal of Hydrology 307:145-163.

Enke, W. and A. Spekat, 1997. Downscaling Climate Model Outputs into Local and Regional Weather Elements by Classification and Regression. Climate Research 8:195-207.

Feddersen, H. and U. Andersen, 2005. A Method for Statistical Downscaling of Seasonal Ensemble Predictions. Tellus A 57:398-408.

Flato, G.M. and G.J. Boer, 2001. Warming Asymmetry in Climate Change Simulations. Geophysical Research Letters 28:195-198.

Fowler, H.J., S. Blenkinsop, and C. Tebaldi, 2007. Linking Climate Change Modeling to Impacts Studies: Recent Advances in Downscaling Techniques for Hydrological Modeling. International Journal of Climatology 27:1547-1578.

Furevik, T., M. Bentsen, H. Drange, I.K.T. Kindem, N.G. Kvamsto, and A. Sorteberg, 2003. Description and Evaluation of the Bergen Climate Model: ARPEGE Coupled with MICOM. Climate Dynamics 21:27-51.

Geurink, J. and R. Basso, 2013. Development, Calibration, and Evaluation of the Integrated Northern Tampa Bay Hydrologic Model. Tampa Bay Water/Southwest Florida Water Management District, Clearwater/Brooksville, Florida.

Geurink, J., R. Basso, P. Tara, K. Trout, and M. Ross, 2006a. Improvements to Integrated Hydrologic Modeling in the Tampa Bay, Florida Region: Hydrologic Similarity and Calibration Metrics. Proceedings of the Joint Federal Interagency Conference April 2-6, 2006, Reno, Nevada.

Geurink, J., K. Trout, and M. Ross, 2006b. Introduction to the Integrated Hydrologic Model. Proceedings of the Joint Federal Interagency Conference April 2-6, 2006, Reno, Nevada.

Goovaerts, P., 1997. Geostatistics for Natural Resources Evaluation. Oxford University Press, New York City, New York, pp. 3-7, 27-36, 127-139, and 152-157.

Graham, L.P., S. Hagemann, S. Jaun, and M. Beniston, 2007. On Interpreting Hydrological Change from Regional Climate Models. Climatic Change 81:97-122, doi: 10.1007/s10584-006-9217-0.

Haan, T.C., 1977. Statistical Methods in Hydrology. The Iowa State University Press, Ames, Iowa, pp. 303-305.

Harbaugh, A.W. and M.G. McDonald, 1996. Programmer's Documentation for MODFLOW-96, an Update to the U.S. Geological Survey Modular Finite-Difference Ground-Water Flow Model. U.S. Geological Survey Open-File Report 96-486, Reston, Virginia.

Hargreaves, G.H. and Z.A. Samani, 1985. Reference Crop Evapotranspiration from Temperature. Applied Engineering in Agriculture 1:96-99.

Hay, L.E., M.P. Clark, R.L. Wilby, W.J. Gutowski, G.H. Leavesley, Z. Pan, R.W. Arritt, and E.S. Takle, 2002. Use of Regional Climate Model Output for Hydrologic Simulations. Journal of Hydrometeorology 3:571-590.

Hidalgo, H.G., M.D. Dettinger, and D.R. Cayan, 2008. Downscaling with Constructed Analogues: Daily Precipitation and Temperature Fields over the United States. California Energy Commission, PIER Energy-Related Environmental Research. CEC-500-2007-123.

Hwang, S. and W.D. Graham, 2013. Development and Comparative Evaluation of a Stochastic Analog Method to Downscale Daily GCM Precipitation. Hydrology and Earth System Sciences 17:4481-4502, doi: 10.5194/hess-17-4481-2013.

Hwang, S., W.D. Graham, A. Adams, and J. Geurink, 2013. Assessment of the Utility of Dynamically-Downscaled Regional Reanalysis Data to Predict Streamflow in West Central Florida Using an Integrated Hydrologic Model. Regional Environmental Change 13(1):S69-S80, doi: 10.1007/s10113-103-0406-x.

Hwang, S., W.D. Graham, J.L. Hernández, C. Martinez, J.W. Jones, and A. Adams, 2011. Quantitative Spatiotemporal Evaluation of Dynamically Downscaled MM5 Precipitation Predictions over the Tampa Bay Region, Florida. Journal of Hydrometeorology 12:1447-1464.

Iizumi, T., M. Nishimori, K. Dairaku, S.A. Adachi, and M. Yokozawa, 2011. Evaluation and Intercomparison of Downscaled Daily Precipitation Indices over Japan in Present-Day Climate: Strengths and Weaknesses of Dynamical and Bias Correction-Type Statistical Downscaling Methods. Journal of Geophysical Research 116:D01111, doi: 10.1029/2010JD014513.

Ines, A.V.M. and J.W. Hansen, 2006. Bias-Correction of Daily GCM Rainfall for Crop Simulation Studies. Agricultural and Forest Meteorology 138:44-53.

Ines, A.V.M., J.W. Hansen, and A.W. Robertson, 2011. Enhancing the Utility of Daily GCM Rainfall for Crop Yield Prediction. International Journal of Climatology 31:2168-2182.

Johnson, F. and A. Sharma, 2012. A Nesting Model for Bias Correction of Variability at Multiple Time Scales in General Circulation Model Precipitation Simulations. Water Resources Research 48:W01504, doi:10.1029/2011WR010464.

Karl, T. and K. Trenberth, 2003. Modern Global Change. Science 302:1719-1722.

Leander, R., T.A. Buishand, B.J.J.M. van den Hurk, and M.J.M. de Wit, 2008. Estimated Change in Flood Quartiles of the River Meuse from Resampling of Regional Climate Model Output. Journal of Hydrology 351:331-343.

Maurer, E.P. and H.G. Hidalgo, 2008. Utility of Dialy vs. Monthly Large-Scale Climate Data: An Intercomparison of Two Statistical Downscaling Methods. Hydrology and Earth System Sciences 12:551-563.

Maurer, E.P., H.G. Hidalgo, T. Das, M.D. Dettinger, and D.R. Cayan, 2010. The Utility of Daily Large-Scale Climate Data in the Assessment of Climate Change Impacts on Daily Streamflow in California. Hydrology and Earth System Sciences 14:1125-1138.

Maurer, E.P., A.W. Wood, J.C. Adam, D.P. Lettenmaier, and B. Nijssen, 2002. A Long-Term Hydrologically-Based Data Set of Land Surface Fluxes and States for the Conterminous United States. Journal of Climate 15(22):3237-3251.

McGregor, J.L., 1997. Regional Climate Modeling. Meteorology and Atmospheric Physics 63:105-117, doi: 10.1007/BF01025367.

Mearns, L.O., I. Bogardi, F. Giorgi, I. Matyasovszky, and M. Palechi, 1999. Comparison of Climate Change Scenarios Generated from Regional Climate Model Experiments and Statistical Downscaling. Journal of Geophysical Research 104:6603-6621.

Mehrotra, R. and A. Sharma, 2012. An Improved Standardization Procedure to Remove Systematic Low Frequency Variability Biases in GCM Simulations. Water Resources Research 48: W12601, doi:10.1029/2012WR012446.

Milly, P.C.D. and P.S. Eagleson, 1988. Effect of Storm Scale on Surface Runoff Volume. Water Resources Research 24(4):620-624.

Murphy, A.J., 1999. An Evaluation of Statistical and Dynamical Techniques for Downscaling Local Climate. Journal of Climate 12:2256-2284.

Panofsky, H.A. and G.W. Brier, 1968. Some Applications of Statistics to Meteorology. The Pennsylvania State University, University Park, Pennsylvania, 224 pp.

Rokicki, R., 2002. Evaluation and Performance of Rainfall Disaggregation Methods for West-Central Florida. M.S. Thesis, University of South Florida, Tampa, Florida.

Ross, M., J. Geurink, A. Said, A. Aly, and P. Tara, 2005. Evapotranspiration Conceptualization in the HSPF-MODFLOW Integrated Models. Journal of the American Water Resources Association 41:1013-1025.

Ross, M., A. Said, K. Trout, P. Tara, and J. Geurink, 2004. A New Discretization Scheme for Integrated Surface and Groundwater Modeling. Hydrological Science and Technology 21:143-156.

Sato, T., F. Kimura, and A. Kitoh, 2007. Projection of Global Warming onto Regional Precipitation over Mongolia Using a Regional Climate Model. Journal of Hydrology 333:144-154.

Schmidli, J., C. Frei, and P.L. Vidale, 2006. Downscaling from GCM Precipitation: A Benchmark for Dynamical and Statistical Downscaling Methods. International Journal of Climatology 26:679-689.

Shepard, D.S., 1984. Computer Mapping: The SYMAP Interpolation Algorithm. *In*: Spatial Statistics and Models, G.L. Gaile and C.J. Willmott (Editors). D. Reidel, Norwell, Massachusetts, pp. 133-145.

Taussky, O. and J. Todd, 2006. Cholesky, Toeplitz and the Triangular Factorization of Symmetric Matrices. Numerical Algorithms 41:197-202.

Vasiliades, L., A. Loukas, and G. Patsonas, 2009. Evaluation of a Statistical Downscaling Procedure for the Estimation of Climate Change Impacts on Droughts. Natural Hazards Earth System Science 9:879-894.

Widmann, M., C.C. Bretherton, and E.P. Salathe, Jr., 2003. Statistical Precipitation Downscaling over the Northwestern United States Using Numerically Simulated Precipitation as a Predictor. Journal of Climate 16:799-816.

Wilby, R.L. and T.M.L. Wigley, 1997. Downscaling General Circulation Model Output: A Review of Methods and Limitations. Progress in Physical Geography 21:530-548.

Wilby, R.L. and T.M.L. Wigley, 2000. Precipitation Predictors for Downscaling: Observed and General Circulation Model Relationships. International Journal of Climatology 20:641-661.

Wilby, R.L., T.M.L. Wigley, D. Conway, P.H. Jones, B.C. Hewitson, J. Main, and D.S. Wilks, 1998. Statistical Downscaling of General Circulation Model Output: A Comparison of Methods. Water Resources Research 34:2995-3008.

Wood, A.W., L.R. Leung, V. Sridhar, and D.P. Lettenmaier, 2004. Hydrologic Implications of Dynamical and Statistical Approaches to Downscaling Climate Model Outputs. Climatic Change 62:189-216.

Wood, A.W., E.P. Maurer, A. Kumar, and D.P. Letternmaier, 2002. Long-Range Experimental Hydrologic Forecasting for the Eastern United States. Journal of Geophysical Research 107:4429, doi: 10.1029/2001JD000659.

Zorita, E. and H. von Storch, 1999. The Analog Method as a Simple Statistical Downscaling Technique: Comparison with More Complicated Methods. Journal of Climate 12:2474-2489.